

# Chapter 1

## Climate Change in Poland in the Past Centuries and its Relationship to European Climate: Evidence from Reconstructions and Coupled Climate Models

**Jürg Luterbacher, Elena Xoplaki, Marcel Küttel, Eduardo Zorita, Jesus Fidel González-Rouco, Phil D. Jones, Marco Stössel, This Rutishauser, Heinz Wanner, Joanna Wibig, and Rajmund Przybylak**

---

J. Luterbacher (✉)

Department of Geography, Climatology, Climate Dynamics and Climate Change,  
Justus-Liebig University Giessen, Giessen, Germany  
e-mail: juerg.luterbacher@geogr.uni-giessen.de

E. Xoplaki

Oeschger Centre for Climate Change Research (OCCR), University of Bern, Bern, Switzerland;  
Institute of Geography, Climatology and Meteorology, University of Bern, Bern, Switzerland;  
The Cyprus Institute, EEWRC, Nicosia, Cyprus

M. Küttel, M. Stössel, and H. Wanner

Oeschger Centre for Climate Change Research (OCCR), University of Bern, Bern, Switzerland

M. Küttel, M. Stössel, and H. Wanner

Institute of Geography, Climatology and Meteorology, University of Bern, Bern, Switzerland

E. Zorita

Institute for Coastal Research, GKSS Research Centre, Geesthacht, Germany

J. Fidel González-Rouco

Dpt. Astrofísica y Ciencias de la Atmósfera, Facultad Ciencias Físicas,  
Universidad Complutense de Madrid, Madrid, Spain

P.D. Jones

Climatic Research Unit, School of Environmental Sciences,  
University of East Anglia, Norwich, UK

T. Rutishauser

Oeschger Centre for Climate Change Research (OCCR), University of Bern, Bern, Switzerland;  
Institute of Geography, Climatology and Meteorology, University of Bern, Bern, Switzerland;  
Unitat d'Ecofisiologia CSIC-CREAF (Center for Ecological Applications and Forestry  
Applications), Universitat Autònoma de Barcelona, Bellaterra, Spain

J. Wibig

Department of Meteorology and Climatology, University of Łódź, Łódź, Poland

R. Przybylak

Department of Climatology, Nicolaus Copernicus University, Torun, Poland

## Abbreviations

AD	Anno Domini
AOGCM	Atmosphere-Ocean General Circulation Model
CCA	Canonical Correlation Analysis
Cc	Centre of Low Pressure
CPC	Climate Prediction Center
CRU	Climatic Research Unit
Bc	Cyclonic Trough
DJF	December January February
EA/WRUS-I	East Atlantic/West Russia Index
EA/WRUS	East Atlantic/West Russia pattern
EOF	Empirical Orthogonal Function
EU2	Eurasia-2 pattern
GCM	Global Circulation Model
ECHAM4	Model name composed from ECMWF and Hamburg
ECHO-G	Model name composed from ECHAM4 and HOPE-G
HadCM3	Hadley Centre Coupled Model, version 3
HOPE-G	Hamburg Ocean Primitive Equation model
IPCC	Intergovernmental Panel on Climate Change
NCAR	National Center for Atmospheric Research
NCEP	National Centers for Environmental Prediction
NAO	North Atlantic Oscillation
NAOI	North Atlantic Oscillation Index
Nc	North Cyclonic Situation
NEc	Northeastern Cyclonic Situation
OASIS	Ocean Atmosphere Sea Ice Soil (model coupling software)
OCER	Oeschger Centre for Climate Change Research
PC	Principal Component
RR	Precipitation
SCAND	Scandinavian pattern
SCAND-I	Scandinavian Index
SLP	Sea Level Pressure
TT	Temperature
UKMO	United Kingdom Meteorological Office

## 1.1 Introduction

The knowledge of climate and its variability during the past centuries can improve our understanding of natural climate variability and also help to address the question of whether modern climate change is unprecedented in a long-term context (Folland et al. 2001; Jansen et al. 2007; Hegerl et al. 2007; Mann et al. 2008 and references therein). The lack of widespread instrumental climate records introduces the need for the use of natural climate archives from ‘proxy’ data such as tree-rings, corals, speleothems and ice cores, as well as documentary

evidence to reconstruct climate in past centuries (see Jones et al. 2009 for a review). The focus of many previous proxy data studies has been hemispheric or global mean temperature (see Jansen et al. 2007; Mann et al. 2008 and references therein), although some studies have also attempted to reconstruct the underlying large-scale spatial patterns of past surface temperature and precipitation changes at continental scales. The principal region where this has been analysed is Europe (e.g. Küttel et al. 2007; Mann et al. 2000; Luterbacher et al. 2004, 2007; Xoplaki et al. 2005; Guiot et al. 2005; Pauling et al. 2006; Riedwyl et al. 2008). Studies indicate that the late twentieth century European climate is very likely warmer than that of any time during the past 500 years. This agrees with findings for the entire Northern Hemisphere. Hemispheric temperature reconstructions do not provide information about regional-scale temperature and precipitation variability such as the intrinsic seasonal patterns of climate change as they have occurred in Europe during the past centuries. High-resolution reconstructions also illuminate key climatic features, such as regionally very mild/cold or wet/dry winters that may be masked in a hemispheric reconstruction. Klimentko and Solomina (2009, this book) present a compilation of climatic variations in the east European plain during the last millennium using different climate proxies. Therefore, regional studies and reconstructions of climate change are critically important when climate impacts are evaluated.

In October 2007 an international conference entitled *The Climate of Poland in Historical Times in Relation to the Climate of Europe* was held in Toruń (Poland). The main aim was to mobilise Polish and international researchers to undertake investigations to improve knowledge about the history of climate in Poland during the past centuries. The outcomes of other results from the conference are published in Parts 2 and 3.

The climate history of Poland is rich and knowledge has increased considerably over the last decades. Information about past weather conditions is found in the collection of more or less systematically written notes about atmospheric phenomena. Weather chronicles in Poland are original notes which have been kept by a number of professors at Cracow University in the second half of the fifteenth century and first half of the sixteenth century (Limanówka 1996). They present visual meteorological observations, performed in most cases sporadically and regularly only in short periods of 1527–1551 (Limanówka 2000) and 1502–1540 (Limanówka 2001). The majority of notes concern the city of Cracow and places with high political, economical, scientific or cultural importance. Bujak (1932) initiated studies related to this topic. The first volume was published by Walawender (1932) and covered the 1450–1586 period. The successive studies of Walawender's team focused on the periods 1587–1647 (Werchracki 1938), 1648–1696 (Namaczyńska 1937) and 1772–1848 (Szewczuk 1939). Publication of the volume covering 1697–1750 prepared by Jukniewicz (1937) was interrupted by the war. As a result, part of the volumes prepared by Werchracki (1938) and Jukniewicz (1937) remained only in the form of short reports and the original volumes were not preserved. The fifteenth and sixteenth centuries are rich with chronicles; in turn the seventeenth century is full of diaries and letters (Limanówka 2001). The different works contain many gaps, which were partially completed by Rojecki (1965). The amount of meteorological

information increases by the end of the seventeenth century, when first instrumental observations became available (Hanik 1972). Long-term climate (mainly temperature and precipitation) reconstructions for the last centuries were presented by Sadowski (1991), Limanówka (1996, 2000, 2001), Trepińska (1997), Bokwa et al. (2001), Majorowicz et al. (2001, 2004), Niedźwiedź (2004), Przybylak et al. (2004, 2005), Büntgen et al. (2007), Šafanda and Majorowicz (2009, this issue) and Majorowicz (2009, this issue). For more details, see Przybylak (2007) and Part 2.

Poland lies in the center of Europe and its climate represents roughly an average climate of Europe (continental climate dominating in eastern Europe and maritime climate occurring in western Europe). Winter temperature in Poland correlates very well with most of Europe as the atmospheric circulation is a main factor influencing climate variations in Poland (see results). The local modifications are rather small because the country is relatively flat. Less than 1% of the Polish area is above 1,000 m and the climatic impact of the Baltic Sea is restricted to a relatively thin belt stretching 50 km along the coast (Woś 1999).

Trenberth (1990) points to the fact that the atmospheric circulation is the main forcing factor for the regional variability of temperature and precipitation. Advective processes exerted by the atmospheric circulation are a crucial factor controlling regional changes of temperature and precipitation. This influence is stronger during winter due to the heat capacity of the underlying surface. Low- and high-frequency variations in air temperatures (year-to-year, decade-to-decade) are far from uniform but occur in distinctive large-scale patterns (Trenberth 1995). Regional or local climate is generally much more variable than climate on a hemispheric or global scale because variations in one region are partially balanced by opposite variations elsewhere (e.g. Mann et al. 2000; Jones and Mann 2004). Indeed a closer inspection of the spatial structure of climate variability, in particular on seasonal and longer time scales, shows that it occurs predominantly in preferred large-scale and geographically anchored spatial patterns (e.g. Baldini et al. 2008). Such patterns result from interactions between the atmospheric circulation and the land and ocean surfaces.

In the context of future climate change one question that is often not considered is the amplitude of regional deviations from the global warming trend, which can be caused by particular sensitivity of the region to external forcing or to internal dynamics, and which can be seasonally dependent. In particular the comparison of regional climate reconstructions and model simulations at regional scales can shed light on the skill of the models to represent realistically the regional variability, and therefore to estimate the amplitude of possible regional multidecadal deviations against the backdrop of a global warming trend (see also Luterbacher et al. 2009; Zorita et al. 2009).

This work attempts to better understand the interannual-to-interdecadal Polish winter precipitation and temperature variability within the reconstruction/observation period in comparison with continental European climate variations covering the last centuries. We will compare the findings with outputs of two GCMs (ECHO-G and HadCM3) and discuss the physical processes behind

those variations. The role of the large-scale atmospheric circulation dynamics/forcing connected with the observed winter temperature and precipitation changes over Poland will be investigated both in the reconstructions and in the model world.

Sections 1.2 and 1.3 briefly describe the datasets (instrumental, reconstructions, GCMs) and the multivariate methods used for this study. The results Section 1.4.1 shows the winter temperature and precipitation evolution over Poland in comparison to Europe back to 1500 within the reconstructions and the ECHO-G and HadCM3 simulations. Further, the relationship between important atmospheric teleconnection patterns and the winter air temperature and precipitation variability over Poland within the last approximately 60 years is investigated in Section 1.4.2. This will provide a first impression on the role of simple circulation indices in driving climate variability over Poland and how the influence changes in space and time. Section 1.4.3 expands on Section 1.4.2 and performs a canonical correlation analysis (CCA) between a new gridded North Atlantic European sea level pressure dataset and Polish winter temperature and precipitation over the 1750–1990 period both using reconstruction/instrumental and model data (ECHO-G and HadCM3). Thus, this part assesses the driving atmospheric large-scale patterns behind recent and past climate anomalies in Poland. The conclusions are presented in Section 1.5.

## 1.2 Data

### 1.2.1 *Instrumental and Reconstructed Data*

Rather than using station data from Poland, we restricted our analysis to gridded high spatial resolution data as this allows us for a better comparison with outputs of GCMs. We used the European mean winter (DJF) surface air temperature reconstructions over land on a  $0.5^\circ \times 0.5^\circ$  grid by Luterbacher et al. (2004, updated using only long temperature series and temperature indices as predictors; Xoplaki et al. 2005; Luterbacher et al. 2007), which are calibrated against the CRU TS2.1 (Mitchell and Jones 2005). The reconstructions are seasonally resolved from 1500 to 1658, when only proxy data (tree-rings, ice cores, documentary-based temperature indices, sea ice information) are available. Thereafter, early instrumental data are also used in the reconstruction approach and the fields are available on a monthly resolution. After around 1760, the main information in these reconstructions comes from early instrumental data (see also Brázdil and Dobrovolný 2009, this issue; Dobrovolný et al. 2009). The reconstructions were used until 1900 and substituted with observation-based data (Mitchell and Jones 2005) thereafter.

Similar as for temperature, seasonal European precipitation was reconstructed by Pauling et al. (2006) back to 1500. Reconstructions are based on a large variety of long instrumental precipitation series, precipitation indices based on documentary evidence (e.g. Brázdil et al. 2005 for a review) and natural proxies that are sensitive

to precipitation signals. The Mitchell and Jones (2005) data were used for calibration and to extend the reconstructions from 1901 to 2002. For more information related to the reconstruction technique and the data used, the reader is referred to the corresponding literature (Luterbacher et al. 2002, 2004; Pauling et al. 2006).

For our purposes we extracted temperature and precipitation for Poland (14.25°E–24.25°E; 49.25°N–54.75°N) consisting of 252 grid points. The area of Poland thus accounts to approximately 4% of all the grid cells of European land areas. The reconstruction method is designed to capture continental-scale temperature and precipitation fields (Luterbacher et al. 2004, 2007; Xoplaki et al. 2005; Pauling et al. 2006). Small-scale variations are not resolved by definition. Therefore, care should be given in the interpretation if a selection of grid points is used.

We used the new gridded  $5^\circ \times 5^\circ$  resolved seasonal sea level pressure (SLP) data produced by Küttel et al. (2009). For the first time terrestrial, instrumental station pressure series and maritime wind information derived from ship log data were combined and statistically extrapolated to a regular grid covering the North Atlantic, Europe and the Mediterranean. This dataset proved to more adequately capture the SLP variability over the North Atlantic than existing sea level pressure reconstructions (e.g. Luterbacher et al. 2002) before the first instrumental SLP measurements in Iceland (Reykjavík in 1821) and Madeira (Funchal in 1850) became available. Furthermore, the new SLP reconstruction does not share any common predictors with reconstructed European temperature (Luterbacher et al. 2004, 2007; Xoplaki et al. 2005) and precipitation reconstructions (Pauling et al. 2006), thus it can be used independently to assess the driving atmospheric patterns behind recent and past climate anomalies. In our analysis we relate this new SLP dataset (40°W–50°E; 20°N–70°N; total consisting of 209 grid points) to winter temperature and precipitation over Poland for the last approximately 250 years using Canonical Correlation Analysis (CCA).

In order to get a first insight on the connection between the atmospheric circulation and the winter (DJF) air temperature and precipitation variability over Poland (using CRU TS3.0 which is an updated version of Mitchell and Jones 2005), a simple correlation (Spearman) analysis of important teleconnection patterns of the Northern Hemisphere is performed. Three anomaly patterns were considered, namely the North Atlantic Oscillation (NAO; Barnston and Livezey 1987), the East Atlantic/Western Russia pattern (EA/WRUS referred to as the Eurasia-2, EU2, pattern by Barnston and Livezey 1987) and the Scandinavian pattern (SCAND; Barnston and Livezey 1987), which are expected to exert an influence on Polish climate.

### 1.2.1.1 North Atlantic Oscillation (NAO)

The North Atlantic Oscillation (NAO) is the most important large-scale mode of climate variability in the Northern Hemisphere. The NAO describes a large-scale meridional vacillation in atmospheric mass between the North Atlantic regions of the subtropical anticyclone near the Azores and the subpolar low pressure system near Iceland (e.g. Wanner et al. 2001 and references therein). Synchronous strengthening (positive NAO phase) and weakening (negative NAO phase) have

been shown to result in distinct, dipole-like climate anomaly patterns between western Greenland/Mediterranean and northern Europe/northeast US/Scandinavia. The monthly derived index (NAOI) is taken from the Climate Prediction Center (CPC) at: <http://www.cpc.ncep.noaa.gov/data/teledoc/telecontents.html>.

### **1.2.1.2 East Atlantic/Western Russia Pattern (EA/WRUS)**

The East Atlantic/Western Russia (EA/WRUS) pattern is one of the two prominent patterns that affect Eurasia during most of the year. This pattern is prominent in all months except June–August, and has been referred to as the Eurasia-2 (EU2) pattern by Barnston and Livezey (1987). In winter, two main anomaly centres, located over the Caspian Sea and western Europe, comprise the EA/WRUS pattern. A three-celled pattern is then evident in the spring and autumn seasons, with two main anomaly centres of opposite sign located over western-northwestern Russia and over northwestern Europe. The third centre, having the same sign as the Russia centre, is located off the Portuguese coast in spring. The monthly derived index (EA/WRUS-I) is taken from the Climate Prediction Center (CPC) at: <http://www.cpc.ncep.noaa.gov/data/teledoc/telecontents.html>.

### **1.2.1.3 Scandinavian Pattern (SCAND)**

The Scandinavian (SCAND) pattern consists of a primary circulation centre, which spans Scandinavia and large portions of the Arctic Ocean north of Siberia. Two additional weaker centres with opposite sign to the Scandinavia centre are located over western Europe and over the Mongolia/western China sector. The SCAND pattern is a prominent mode in all months except June and July and has been previously referred to as the Eurasia-1 pattern by Barnston and Livezey (1987). The positive phase of this pattern is associated with positive height anomalies, sometimes reflecting major blocking anticyclones, over Scandinavia and western Russia, and negative anomalies over the Iberian Peninsula and northwestern Africa. The SCAND pattern plays a considerable role in precipitation variability over Europe (Wibig 1999). The corresponding monthly index (SCAND-I) stems from the CPC at: <http://www.cpc.ncep.noaa.gov/data/teledoc/telecontents.html>.

## ***1.2.2 Model Data***

### **1.2.2.1 ECHO-G Temperature and Precipitation Data**

ECHO-G is a coupled atmosphere-ocean general circulation model (AOGCM), consisting of the ECHAM4 atmospheric general circulation model and the Hamburg Ocean Primitive Equation model HOPE-G, which includes a dynamic-thermodynamic sea-ice model with snow cover. Both components were developed at the Max-Planck



Institute for Meteorology in Hamburg and coupled with the OASIS-Software. The atmospheric component ECHAM4 has a horizontal resolution of T30 (approx.  $3.75^\circ \times 3.75^\circ$  longitude/latitude) and 19 levels along the vertical direction, five of them located above 200 hPa, the highest being 10 hPa, thus having a rather coarse resolution of the stratosphere. The oceanic component HOPE-G has a resolution of approx.  $2.8^\circ \times 2.8^\circ$  longitude/latitude, with a decrease in meridional grid point separation towards the equator to a value of  $0.5^\circ$ . This enables a more realistic representation of equatorial ocean currents. HOPE-G has 20 levels along the vertical direction. Due to the interactive coupling between ocean and atmosphere and the coarse model resolution, ECHO-G needs a constant mean flux adjustment to avoid a significant climate drift. Thus additional fluxes of heat and freshwater are applied to the ocean. This flux adjustment is constant in time and its global integral vanishes. In this comparison, the ‘Erik-the-Red’ run of ECHO-G is used (von Storch et al. 2004; González-Rouco et al. 2006). This simulation includes natural (solar irradiance and the radiative effect of volcanic eruptions) and anthropogenic (greenhouse gases) forcing over the period 1000–1990.

For the CCA (see below) between the large-scale winter atmospheric circulation and Polish winter temperature and precipitation variability back to 1750 we used the same spatial area as for the reconstructions/instrumental data set. For SLP we selected 350 grid points representing the area  $40^\circ\text{W}$ – $50^\circ\text{E}$ ;  $25^\circ\text{N}$ – $70^\circ\text{N}$  while for temperature and precipitation only six grid points representing Poland were chosen.

### 1.2.2.2 HadCM3 Temperature and Precipitation Data

As ECHO-G, HadCM3 is a state-of-the-art AOGCM. Unlike ECHO-G, no flux adjustment to prevent large climate drifts is applied in the model HadCM3. However, a small long-term climate drift is still present, the magnitude of which is estimated from a long control run. This drift is then corrected from the temperature data of the present simulation (Tett et al. 2007). The atmospheric component HadAM3 is a version of the United Kingdom Meteorological Office (UKMO) unified forecast and climate model with a horizontal grid spacing of  $2.5^\circ$  (latitude)  $\times$   $3.75^\circ$  (longitude) [the T-resolutions apply only to spectral models]. HadAM3 is a finite-difference model and has 19 levels along the vertical direction. The ocean component has 20 levels with a spatial resolution of  $1.25^\circ \times 1.25^\circ$  degrees thus resulting in six ocean grid cells to one atmosphere grid cell. The resolution is higher near the ocean surface, making it therefore possible to represent important details in oceanic current structures. The sea ice model uses a simple thermodynamic scheme including leads and snow-cover. In this study, two HadCM3 runs were merged: a natural-forcings run from 1500 to 1749 and an all-forcings run spanning the period 1750–1999. The natural-forcings run is driven by prescribed changes in volcanic forcing, solar irradiance and orbital forcing, while anthropogenic forcing factors were fixed at estimated pre-industrial values. The all-forcings run on the other hand is driven by prescribed changes in volcanic forcing, solar irradiance, orbital forcing, greenhouse gases, tropospheric sulphate aerosol, stratospheric ozone and land-use/land-cover.



For the CCA between the large-scale winter atmospheric circulation and Polish winter temperature and precipitation variability back to 1750 we used the same spatial area as for the reconstructions/instrumental data set. For SLP we selected 525 grid points whereas for temperature and precipitation nine grid points representing Poland were extracted.

There are relevant differences in the implementation of some of the external forcings in both models. The most important comprise the volcanic forcing. Whereas in ECHO-G the overall radiative effects of the volcanic aerosols on the radiation balance is implemented as a global change in the effective solar constant, in HadCM3 the prescribed radiative properties of the volcanic aerosols are explicitly represented for several latitudinal bands. Also, in HadCM3 the effect of aerosols in the short-wave and infrared spectral bands is treated separately, whereas in ECHO-G only the integrated change in the radiative forcing is parameterised within the solar forcing. The amplitude of the past changes of solar irradiance is also slightly different in both model simulations. In the ECHO-G simulation the changes between present and the Late Maunder Minimum amount to 0.3% of the total solar constant, whereas in the HadCM3 simulation the solar irradiance is assumed to have changed by 0.25% (Tett et al. 2007) between these two periods.

Another difference is that the HadCM3 simulation is also driven by tropospheric aerosols in the twentieth century. Its radiative forcing is most strongly felt in Northern summer in the twentieth century. The ECHO-G simulation does not include tropospheric aerosols.

Finally, the forcings in the HadCM3 simulation include changes in the land-use, which in Europe have been especially large in the past centuries. The increasing surface albedo associated with deforestation and expanding agricultural lands leads to more shortwave radiation being reflected back to space and, other factors remaining unchanged, to lower surface temperatures. This effect is missing in the ECHO-G simulation, which does not consider past land-use changes.

In general, the implementation of some of the forcings in the HadCM3 runs, specially volcanic and tropospheric aerosols, is a priori more realistic than in the ECHO-G runs.

## 1.3 Methods

### 1.3.1 *Canonical Correlation Analysis (CCA)*

To assess the connection between the new gridded large-scale SLP data of Küttel et al. (2009) and Polish winter temperature and precipitation both in the reconstruction/instrumental and model world, we calibrated a downscaling model using CCA in the empirical orthogonal function (EOF) space and subsequently validated this model by means of cross-validation (e.g. Michaelson 1987). To be consistent with the length of the three different data sets, we applied CCA over the common period 1750–1990. Only a short overview of the methods used is provided here, for

a detailed description of the methodology the reader is referred to Barnett and Preisendorfer (1987), Wilks (1995) and von Storch and Zwiers (1999). Before performing the CCA, the original data were projected onto their EOFs retaining only a limited number of them, accounting for most of the total variance in the datasets. As a preliminary step to the calculation of EOFs, the annual cycle was removed from all station and grid point time series by subtracting from each winter value the 1750–1990 long-term mean. The gridded predictor data were then weighted by multiplying with the square root of the cosine of latitude to account for the latitudinal variation of the grid area (North et al. 1982; Livezey and Smith 1999). A further step to ensure the stationarity of the variables needed for the calculation of EOFs and CCA was to detrend the time series. A standard linear least square fit method has been used as described for example by Edwards (1984). After the diagonalisation of the covariance and cross-correlation matrices during the EOF and CCA processes, the long-term trends were recovered by regressing the original datasets onto their EOFs or canonical vectors as in Busuioc and von Storch (1996). This provides estimations of the principal components and canonical series with long-term variability and trends. We have used five EOFs of Polish temperature and Polish precipitation as well as of large-scale SLP for the reconstructions and the model data. To calculate the statistical models during cross-validation in all exercises we used all five canonical vectors. The cross-validation was applied by discarding one winter from the data set in each step and then predicting them, based on the remaining data. This process was repeated for each winter in the 1750–1990 record (e.g. von Storch and Zwiers 1999). The performance of the statistical model was evaluated by calculating the correlation between the predicted and the raw data. The correlation provides a measure of time concordance in the series.

## 1.4 Results and Discussions

### *1.4.1 Comparing Winter Temperature and Precipitation Over Poland and European Land Areas in Reconstructions and in the Model World*

This section characterises the seasonal temperature and precipitation evolution of Poland extracted from Luterbacher et al. (2004) and Pauling et al. (2006) covering the past 500 years. It highlights the relation between the temperature/precipitation evolution over Poland compared to the European average. This will shed light on the importance of that part of Europe in explaining seasonal temperature and precipitation changes at continental scales and how stable those connections are through time. Apart from multiproxy temperature and precipitation reconstructions updated with new gridded instrumental data (Mitchell and Jones 2005), we also use simulation data from the coupled global climate models ECHO-G (von Storch et al. 2004; González-Rouco et al. 2006) and HadCM3 (Tett et al. 2007). The rationale behind this comparison is on the one hand to test the realism of the models in simulating

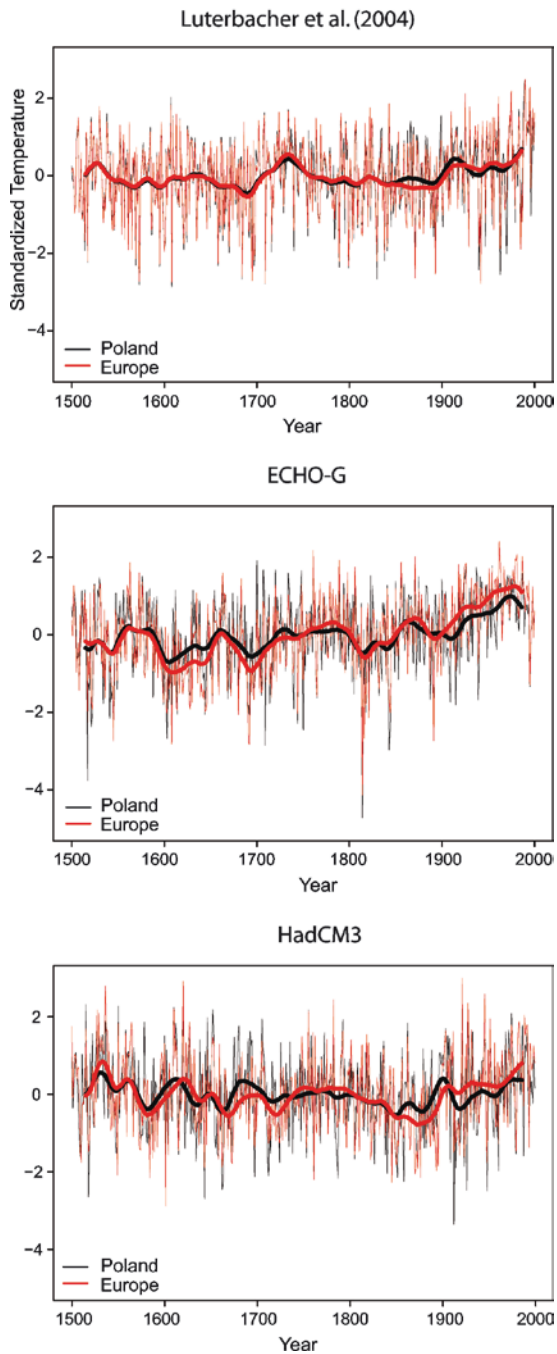
the subcontinental regional variability at multidecadal time scales. On the other hand, this analysis will help to support specific aspects of the reconstructions with model results that may possibly be uncertain, as for instance the robustness of the large- to regional-scale links found in the instrumental period and their stability with time in a multicentennial context.

Figure 1.1 shows the standardized winter (DJF) temperature evolution of Poland and European land areas (excluding Poland) over the past 500 years presented by Luterbacher et al. (2004) and as simulated by the ECHO-G and HadCM3 models.

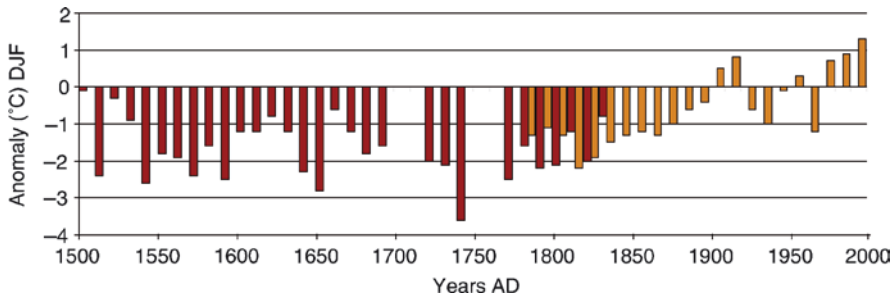
The correlation (at interannual and multidecadal time scales) between reconstructed Poland and European mean temperatures (excluding the grid points representing Poland) over the full 500 year period is 0.96 (Fig. 1.1 top row). Similar high values are found if only twentieth century instrumental data are used. It shows the generally below normal winter conditions through a large part of the so-called 'Little Ice Age' with lowest values within the Late Maunder Minimum period (late seventeenth/early eighteenth century), a short warming period until the late 1730s (see Luterbacher et al. 2004, 2007; Jones and Briffa 2006), followed by colder conditions again. The twentieth century instrumental period is characterised by a temperature increase with the very likely highest values at the turn of the twenty first century (see also Luterbacher et al. 2004, 2007 for details). The very strong relationship between Polish winter and European temperatures both at interannual and interdecadal time scale is of major interest since some of the longest temperature proxy information stem from Poland (e.g. Sadowski 1991; Trepínska 1997; Bokwa et al. 2001; Majorowicz et al. 2004; Przybylak et al. 2005; Büntgen et al. 2007; Šafanda and Majorowicz 2009; Majorowicz 2009; see also Parts 2 and 3 of this book) which can improve European seasonal mean temperature reconstructions significantly.

Figure 1.2 presents decadal averaged winter (DJF) air temperature anomalies for the last 500 years for Poland with respect to the 1901–1960 reference period (Przybylak et al. 2005). Reconstructed 10-year mean winter air temperatures for parts of Poland based on documentary sources (that have not been used by Luterbacher et al. 2004, thus can be considered as independent) covering the period from 1501 to 1840 (Przybylak et al. 2005) were generally lower than the air temperatures occurring in the twentieth century (see detailed description and presentation of available long-term climate time series from Poland presented in Part 2 on Chapter 5, Przybylak 2009). The coldest winters, on average, occurred in the decade 1741–1750 (anomaly  $-3.7^{\circ}\text{C}$  with respect to the 1901–1960 reference period). The warm period in the 1730s shown in Fig. 1.1 (see also Jones and Briffa 2006) is not present in Poland's temperature reconstruction (Fig. 1.2). According to Przybylak et al. (2005), winters in this decade were colder by about  $2^{\circ}\text{C}$ . In Czech Lands (Brázdil 1996) they were near the long-term average.

Large negative anomalies were observed in the following decades: 1541–1550, 1571–1580, 1591–1600, 1641–1650, 1651–1660 and 1771–1780. On the other hand, warm winters, on average, occurred in the first and third decades of the sixteenth century, and in the seventeenth century, except for the periods from 1630 to 1660 and from 1680 to 1700. A visual comparison of these results with the Luterbacher et al. (2004) European mean reconstruction (see Fig. 1.1, top panel) indicates that there is generally good agreement mainly for the first approximately 200 years with



**Fig. 1.1** Standardized winter mean temperatures of Poland (black line) and European land areas (excluding Poland, red line) 1500–2000 as reconstructed by Luterbacher et al. (2004, top panel), simulated by ECHO-G (von Storch et al. 2004; González-Rouco et al. 2006, middle panel) and HadCM3 (Tett et al. 2007, bottom panel). The thick lines denote the 30-yr running means



**Fig. 1.2** Decadally averaged winter (DJF) air temperature anomalies for Poland with respect to the 1901–1960 reference period. *Dark red bars* present reconstructions based on documentary evidence (Przybylak et al. 2005), *Orange bars* (observation from Warsaw) are taken from Lorenc (2000)

below normal conditions. However, differences are found for instance at times when the lowest and highest winter temperatures occurred: documentary evidence from Poland indicates that in the seventeenth century the coldest winters occurred rather in the first half of the Late Maunder Minimum (Przybylak et al. 2005). A major difference is also the European winter warming trend starting in the late seventeenth century until the first decades of the eighteenth century (Fig. 1.1, top panel) (Luterbacher et al. 2004, 2007) which is not supported by the study of Przybylak et al. (2005) which either has gaps in the series or points to colder conditions. Despite these differences the estimated winter temperatures lay both within the uncertainty ranges of each other (not shown).

The match between the grid points representing Poland and Europe mean winter temperature in the model (in the corresponding model grid-cells) is similar to the reconstructions (Fig. 1.1). The correlations at interannual to multidecadal time scales are highly significant for ECHO-G and HadCM3, indicating that the correlation across space is in agreement in the models and the reconstructions. The ECHO-G winter temperature for Europe and Poland points to a slight overall warming from 1500 to the late 20th century, with minima around the end of the seventeenth and the beginning of the nineteenth centuries. There is a discernible acceleration of the warming trend within the twentieth century that leads to the highest temperatures at the end of the century. The overall long-term trend appears somewhat larger than in the reconstructions. The European/Poland winter temperature evolution within the HadCM3 model does not indicate an overall trend within the last half millennium and the warming in the twentieth century seems to be smaller than in ECHO-G and in the reconstruction/observations. The HadCM3 simulation does not display distinctive minima around the Late Maunder Minimum period. Concerning the interannual variability, the reconstructions display larger variations than in both simulations, in particular for the European average temperatures.

One reason for the stronger coherency in the reconstructions/instrumental data could be the inclusion of land and ocean grid points in the model simulations. Considering Fig. 1.3 (see below), both models and the instrumental data yield a

very similar spatial correlation pattern between Polish mean temperature and the European field, whereas the reconstructions display longer spatial coherence, in particular in the zonal direction (in the meridional direction all four data sets seem quite similar). One speculation could be that in the reconstructions the variations in the zonal circulation have been more effective in modulating the winter temperature over the continent, whereas in the model it seems not to be so much the case. Possibly, this is linked with the inability of both models to produce warm episodes such as in 1730 (Jones and Briffa 2006; Zorita et al. 2009), and with the inability of models in general to reproduce the low-frequency variability of the NAO in the twentieth century (Osborn 2004). In summary the model swings of the NAO would be too short-lived and too weak, and this reflects in lower spatial temperature coherence, in particular in the zonal direction. It might be worth exploring this in more detail in future studies.

In general the HadCM3 simulation displays less long-term variability than the ECHO-G simulation, but there are also clear differences between both simulations and the reconstructions. The differences between model simulations can be due to the different magnitude of the changes in past solar forcing that are smaller in the HadCM3 simulations than in the ECHO-G simulation. However, it is difficult to explain some of these differences by invoking the external forcing alone. In the case of ECHO-G the total external forcing may be overestimated, due to the missing cooling effect of tropospheric aerosols in the twentieth century and the coarse representation of the volcanic forcing (in the model it can only induce cooling, whereas in reality tropical volcanic eruptions may induce a transient winter warming at middle and high latitudes due to atmospheric circulation anomalies, (Stenchikov et al. 2006). Also the magnitude of the long-term past solar changes is uncertain. One difference between the simulations and the reconstruction that is not likely to be dependent on the prescribed forcing is the level of interannual variability, which is larger in the reconstructions. A possible reason is that the reconstructed data are basically the result of a linear combination of a limited number of local proxy and documentary records, whereas in the models, the grid-cell values represent spatial averages over the whole grid-cell. This sampling effect alone would cause higher interannual variations in the reconstructions, although it is difficult to quantify whether or not it can completely explain the gap between simulations and reconstructions.

Figure 1.3 presents the spatial Pearson correlation maps between the average winter temperature of Poland (14.25°E–24.25°E; 49.25°N–54.75°N) and European land areas for the past 500 years (400 years reconstructions, the last 100 years gridded CRU data) and for the two GCMs. Approximately, 20 Polish station series are included in the gridded CRU TS3.0 dataset.

Except for the Icelandic area and the very southeast, the correlation between Poland winter temperature and European grid cells is highly significant. Thus, Fig. 1.3 underlines the strong connection between the area of Poland and most European areas (Poland excluded, Fig. 1.1) and the strong consistency between reconstructions/instrumental and model data.



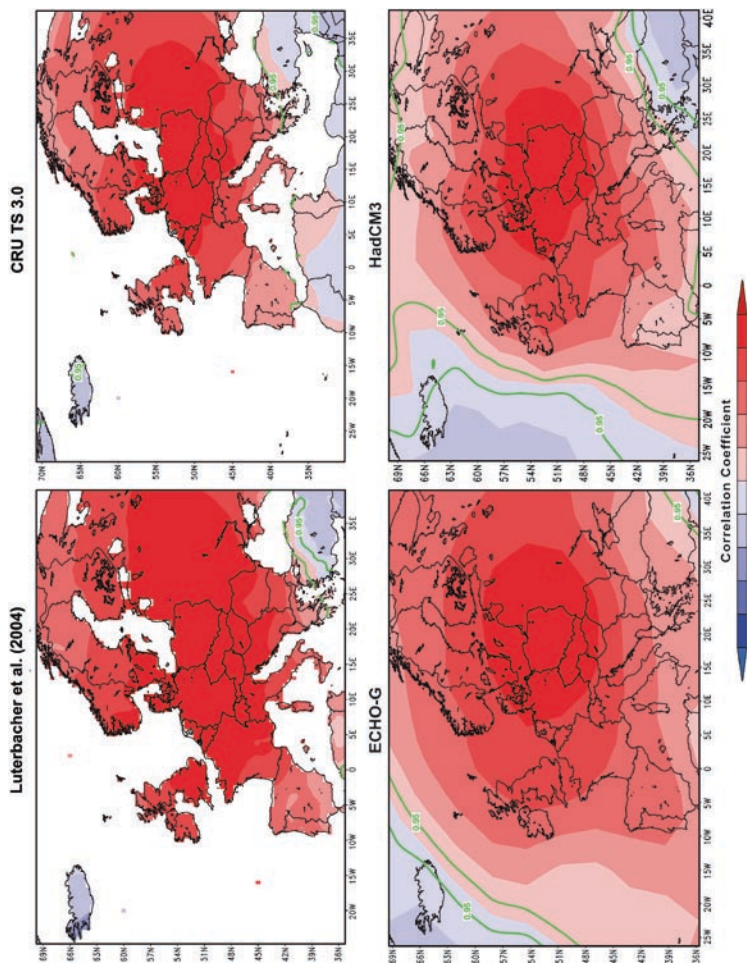


**Fig. 1.3** (top left) Spatial correlation maps between winter temperature averaged over Poland (14.25°E–24.25°E; 49.25°N–54.75°N) and European land areas over the past 500 years (Luterbacher et al. 2004), (top right), as top left but for the instrumental period 1901–2006 (using CRU TS3.0); (bottom left) Spatial correlation maps between winter temperature averaged over Poland (15°E–22.5°E; 50.625°N–54.375°N) and Europe for the period 1500–1990 within the ECHO-G model (von Storch et al. 2004; González-Rouco et al. 2006); (bottom right) as bottom left but for 15°E–22.5°E; 50°N–55°N, the period 1500–1999 and the HadCM3 model (Tett et al. 2006). The significant areas (95% level) are marked in green contours



This result supports the ability of models to represent the regional climate variations in the frame of the European scale. The similar correlation patterns obtained from model and reconstructed and instrumental data indicates that the spatial correlation structure of the temperature field is well captured by the models. In addition, some minor features found in the reconstruction and in observations such as the smaller areas of negative correlations over Iceland and the eastern Mediterranean are also supported by both models at multicentennial time scales.

Precipitation is spatially and temporally more variable than temperature. However, the reconstructed winter precipitation over Poland (Pauling et al. 2006) also agrees very well with the entirety of Europe (Poland excluded; Fig. 1.4, top panel). The correlation at interannual and multidecadal time scales accounts for 70% of the total variance. The agreement is smaller in the model world (ECHO-G: interannual winter 0.19; multidecadal 0.41; HadCM3 interannual winter 0.04; multidecadal 0.39). One reason for the differences between reconstructions and models may be that in the mean model precipitation the whole Mediterranean Sea is included that returns negative correlations with Polish precipitation, whereas the average mean in the reconstruction only includes land areas. Another reason might be due to the reduced number of PCs reconstructed. The principal component regression used for the reconstructions may impose a spatial homogeneity upon the reconstructed data that is not so strongly present in the instrumental data. Very likely this effect is stronger for precipitation where the EOF filtering would be relatively stronger because of the noisy character of precipitation.

There is no overall trend visible in the precipitation reconstructions (Fig. 1.4). The discrepancies between Poland and Europe (excluding Poland) can be found in the early twentieth century with wetter (drier) conditions in Poland (Europe). The end of the twentieth century is characterised by wetter overall European winter conditions but lower values in Poland.

The model simulations do not display clear long-term trends for winter precipitation either. Only the ECHO-G simulation shows a small non-significant trend along the 500 year period towards wetter conditions. The low-frequency variability in the model simulations is comparable to the one in the reconstructions, but the interannual variability is larger in both simulations, in particular in the early two centuries. The reconstructed interannual variability increases along the 500 year period, but this could be due to missing information in the proxy and documentary records in the early period. In general, the model simulation indicates quite stable precipitation conditions over the full half millennium. Precipitation is known to be a variable with a high level of internal variations, and more so at regional scales, and it is more difficult to detect the influence of external forcing. This happens also in simulations for future climate with larger variations in the external forcing than in the past millennium (Barnett et al. 2004).

Figure 1.5 presents the spatial Spearman correlation maps between the average winter precipitation of Poland and European land areas for the past 500 years (Pauling et al. 2006), the last 100 years of gridded CRU TS3.0 data and within the two GCMs. The spatial correlation patterns are less homogenous compared to winter temperature conditions (Fig. 1.3) but generally indicate similar results. As in the

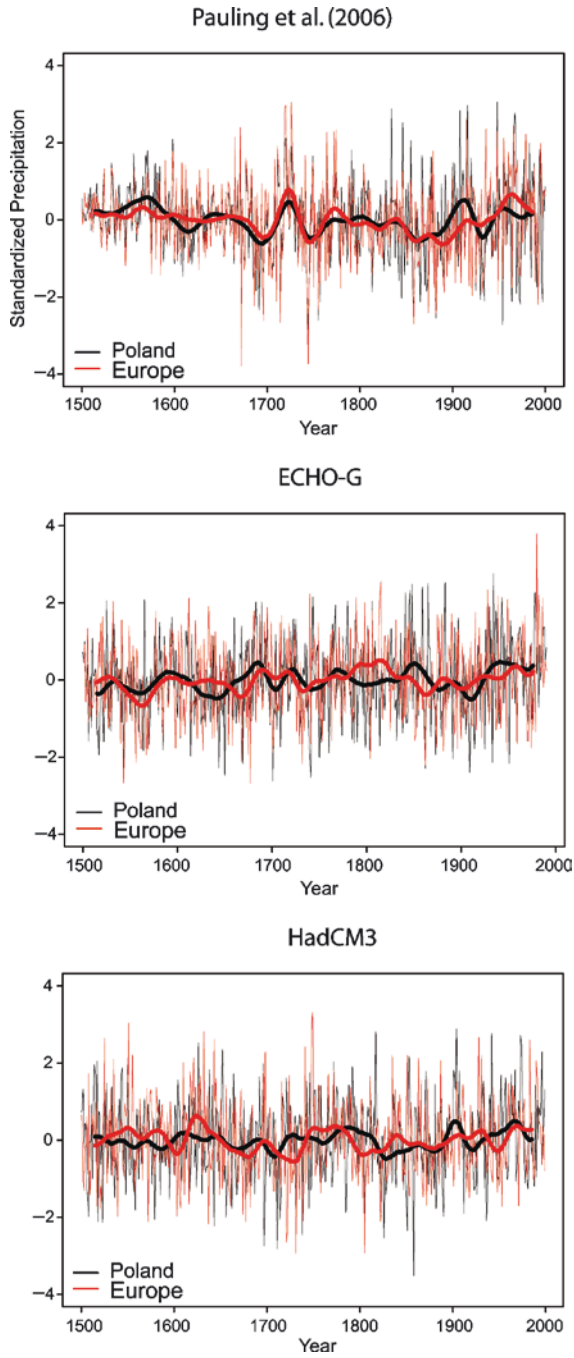
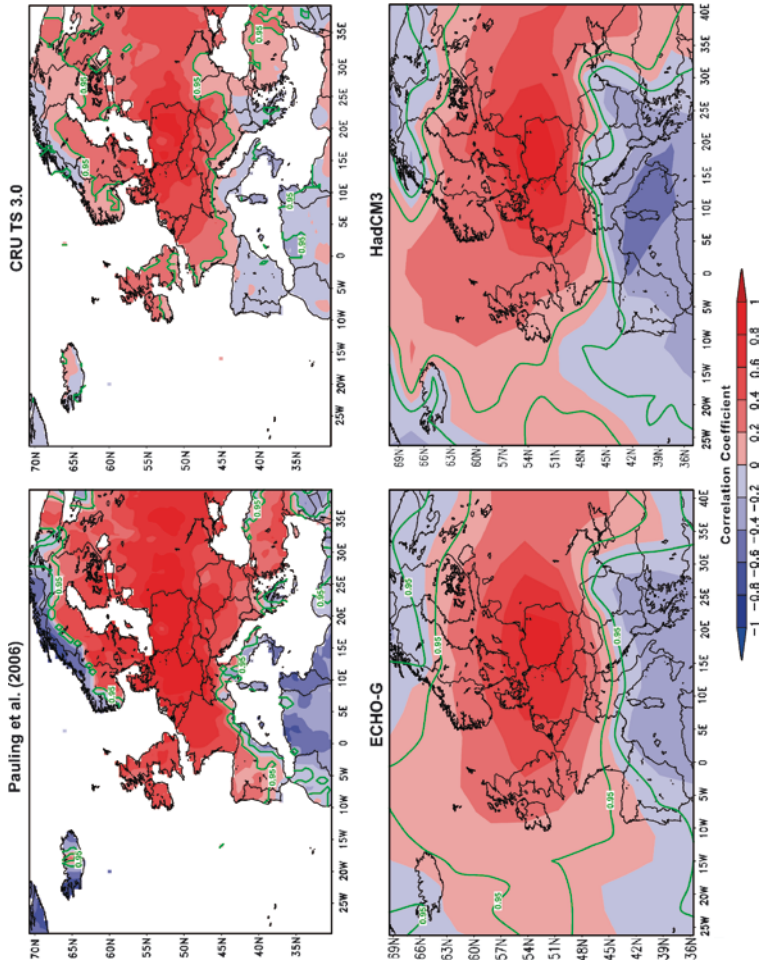


Fig. 1.4 As Fig. 1.1, but for precipitation



**Fig. 1.5** (*top left*) Spatial correlation maps between winter precipitation averaged over Poland (14.25°E–24.25°E; 49.25°N–54.75°N) and European land areas over the past 500 years (Pauling et al. 2006), (*top right*), as top left but for the instrumental period 1901–2006 (using CRU TS3.0); (*bottom left*) Spatial correlation maps between winter precipitation averaged over Poland (15°E–22.5°E; 50.625°N–54.375°N) and Europe for the period 1500–1990 within the ECHO-G model (von Storch et al. 2004; González-Rouco et al. 2006); (*bottom right*) as bottom left but for 15°E–22.5°E; 50°N–55°N, the period 1500–1999 and the HadCM3 model (Tett et al. 2006). The significant areas (95% level) are marked in green contours

case of winter temperature the spatial patterns of the reconstructions/last 100 year instrumental data and GCMs are consistent with significant positive correlations generally over northern and eastern Europe and negative correlations in the Mediterranean area. The signal is weaker than temperature but still large parts of Europe show coherence with mean Polish winter precipitation.

The spatial coherency of precipitation in the models seems more similar to the observations, whereas the reconstructions display high correlations over longer distances. This could be due to the PC basis of the reconstructions (see above).

The next section sheds some light on the relation between selected atmospheric teleconnection indices and Polish winter temperature and precipitation.

### ***1.4.2 Spatial Correlation Analysis Between Polish Winter Precipitation and Temperature with Teleconnection Indices***

For the period 1950–2006 correlations between the Polish winter temperature and precipitation (using CRU TS 3.0, of gridded CRU TS3.0 data) and the NAOI (e.g. Barnston and Livezey 1987), SCAND-I (Barnston and Livezey 1987) and the EA/WRUS-I (Barnston and Livezey 1987) were calculated (Fig. 1.6).

The spatial correlation pattern demonstrates that winter temperature over Poland is significantly positively correlated with the North Atlantic Oscillation Index (NAOI,  $p < 0.05$ ). More than 50% of the winter temperature variations can be accounted for by the influence of this index. For the longer period (1780–1990) Przybylak et al. (2003) found approximately a twice as small influence of the NAO on winter temperature in Warsaw. The spatial correlation map between the winter NAO and winter precipitation over Poland reveals a dipole pattern with positive (negative) correlations in the north (south). The NAO explains approximately 25–30% of the winter precipitation variations in the northwest and southeast of Poland (Fig. 1.5 bottom). Winter precipitation in Poland was also analysed in relation to circulation patterns at 500 hPa level by Wibig (1999). Monthly precipitation totals from 12 Polish stations from the period 1951–1990 were correlated with circulation patterns defined as rotated principal components of the 500 hPa geopotential heights in the Euro-Atlantic sector and generally agree with the findings in Fig. 1.6.

The spatial correlation can be explained by typical and dominant winter circulation patterns in Europe. The highly correlated areas (see also Figs. 1.3 and 1.5) indicate a clear influence of zonal circulation conditions, either through a westerly component related to mild and wet air masses from the Atlantic or through cold and mostly dry continental air from east (negative phase of the NAO or strong western Russian or Baltic high pressure system). This zonal pattern indicates a strong influence of the NAO (see also Fig. 1.6) on the European continent in winter with above normal precipitation between the British Isles and eastern Europe in positive phases (e.g. Hurrell 1995; Jones et al. 2003; Baldini et al. 2008). In periods of a negative

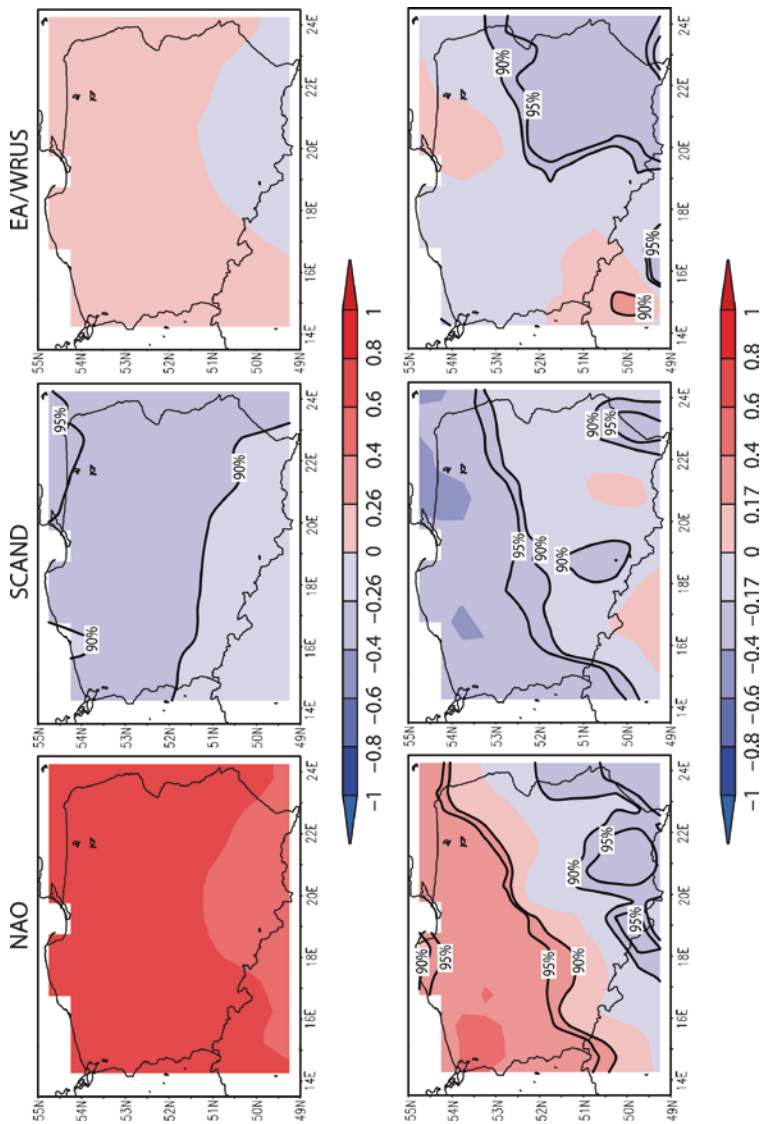


**Fig. 1.6** Spatial correlation between NAO (*left*), SCAND (*middle*) and EA/WRUS (*right*) teleconnection indices and the  $0.5^\circ \times 0.5^\circ$  gridded CRU TS 3.0 surface air temperature (*top row*) and precipitation (using CRU TS3.0 *bottom row*) over the period 1950–2006 (indices downloaded from <http://www.cpc.ncep.noaa.gov/data/teledoc/teleconents.shtml>, accessed July 12th 2008). For temperature the Pearson product-moment and for precipitation the Spearman rank correlation coefficient (e.g. Wilks 1995) was applied. Significant areas at the 90% and 95% significance levels are indicated. Note, in the NAO/temperature panel all areas are statistically significant at the 95% level

NAOI, more moisture is conveyed to the western Mediterranean whereas weaker westerly winds allow a stronger influence of cold and dry continental air masses in central and eastern Europe, including Poland. The congruence of precipitation amounts between Poland and the area between the English Channel and Russia could also be demonstrated in Stössel (2008), where the area between France and the Baltic Sea was calculated to be the most representative for explaining European winter precipitation.

The correlation between SCAND-I and Polish temperature in winter is generally negative, though significant ( $p < 0.1$ ) only in the central and northern parts. In case of a positive SCAND-I, a strong positive pressure anomaly is centred over Scandinavia and western Russia and negative anomalies over the Iberian Peninsula connected with anomalous easterlies and thus cold and dry airflow over the area of interest. Positive (negative) SCAND-I go along with negative (positive) winter precipitation anomalies in the northern parts of the country. SCAND explains around 25–30% of the winter precipitation variations in the northern parts of the country, while only 5–10% of winter temperature variations can be related to the SCAND pattern. The mountainous southern part returns mostly non-significant results.

The EA/WRUS pattern does not seem to exert any significant influence on Polish winter temperature (Fig. 1.6 top). Concerning precipitation, a significant contribution of the EA/WRUS influence on Polish winter precipitation can be found in the southeastern parts of the country (Fig. 1.6 bottom).

Wibig (2009) has shown that mean winter minimum, maximum and average daily temperature calculated from station data (23 stations from Poland) as well as numbers of frost days in winter (days with minimum temperature equal or below 0°C) and ice days (days with maximum temperature equal or below 0°C) correlate positively with the NAO and EA indices and negatively with the SCAND-I.

Differences of sea level pressure (based on CRU grid point pressure data) and 500 hPa levels (taken from NCEP/NCAR dataset) between the 10 wettest and the 10 driest, as well as between the 10 hottest and the 10 coldest months were also analysed (Wibig 2004). During wet periods the pressure gradient over Europe was stronger and the storm tracks over the North Sea and northern Scandinavia were more frequent than during the dry ones, when the blocking situations over central Europe occurred more often. The deep Icelandic Low accompanied the inflow of warm air from the west during warmer winters. Degirmendžić et al. (2004) analyzed the sensitivity of air temperature and precipitation variations to circulation variations described by sea-level pressure in the centre of Poland (52.5°N, 20°E) and geostrophic wind calculated from meridians 45°N and 65°N and the latitudes at 10°E and 30°E. By using multiple regression it was shown that these three factors (SLP at selected grid point and both components of geostrophic wind) explain up to 77% and 44% of temperature and precipitation variability respectively. Twardosz and Niedźwiedz (2001) have shown that high precipitation events in Poland are most frequent during the northeastern cyclonic situation (NEc), north cyclonic situation (Nc), cyclonic trough (Bc) and centre of low pressure (Cc) according to typology by Niedźwiedz (1992, 2004).

Rosenzweig et al. (2008) showed that changes in biological and physical systems consistently occur in regions of observed temperature increase that itself



cannot be explained by natural climate variations alone. Long-term, regional-scale dynamical analyses of temperature and precipitation variability are essential for the detection of impacts and adaptation of ecosystems (Ahas et al. 2002; Menzel et al. 2006; Rutishauser et al. 2008). Often the regional impacts are related to atmospheric circulation patterns such as the NAO (Scheifinger et al. 2002; Aasa et al. 2004; Bednorz 2004; Menzel et al. 2005; Sinelschikova et al. 2007). In years with strong positive NAOI in both winter and spring, the latitudinal gradients of spring phases are smaller making the spatial pattern more uniform (Menzel et al. 2005). There is a large body of evidence that changes in general circulation impact regional temperature patterns in Poland and this, in turn, will induce changes in the timing of ecosystem processes (Bednorz 2004; Aasa et al. 2004; Menzel et al. 2005, 2006). Changes in snow cover, plant vegetation activity onset and changes in bird migration and pollen season are a few indications of climate change impact evidence. Fourteen out of 16 migratory bird species in western Poland tend to arrive earlier in the 1990s than in the 1910s (Tryjanowski et al. 2002). Tryjanowski and Sparks (2008) showed that the arrival time of white stork (*Ciconia ciconia*) in Poland during the period 1983–2003 had an impact on the duration of occupied nests and thus greater productivity. Stach et al. (2008) suggest that the severity of the birch pollen season in Poland is related to the NAOI for the period 1995–2005. However, the more remote site from the Baltic Sea, Cracow, showed only a very limited correlation with the NAO. These examples show the overall impact of climate change on regional ecosystems and human health (Stach et al. 2008) but also highlight the strong local modifications by causes not related to climate.

### ***1.4.3 CCA Between Winter Large-Scale Atmospheric Circulation and Winter Climate Variability in Poland Back to 1750 Using Reconstructions/Instrumental Data and GCMs***

#### **1.4.3.1 CCA SLP-Polish Winter Temperature**

The interannual to interdecadal covariability between Polish winter temperature and large-scale atmospheric circulation during the period 1750–1990 is presented using canonical patterns for the reconstructions/instrumental data and for the two GCMs. The results focus on the first CCA mode, since it captures most of the Polish temperature variability. Spatial patterns and expansion coefficients of the modes are presented in Figs. 1.7, 1.8 and 1.9. The variance that is explained by the first CCA pattern (Fig. 1.7) is approximately 35% for SLP and 89% of Polish winter temperature. This pair exhibits a canonical correlation of 0.79 for the unfiltered data.

The first canonical map of SLP shows the well-known dipole pattern with positive values (related to positive normalised time components in Fig. 1.7 bottom left) south of approximately 50°N and negative SLP anomalies north of it.



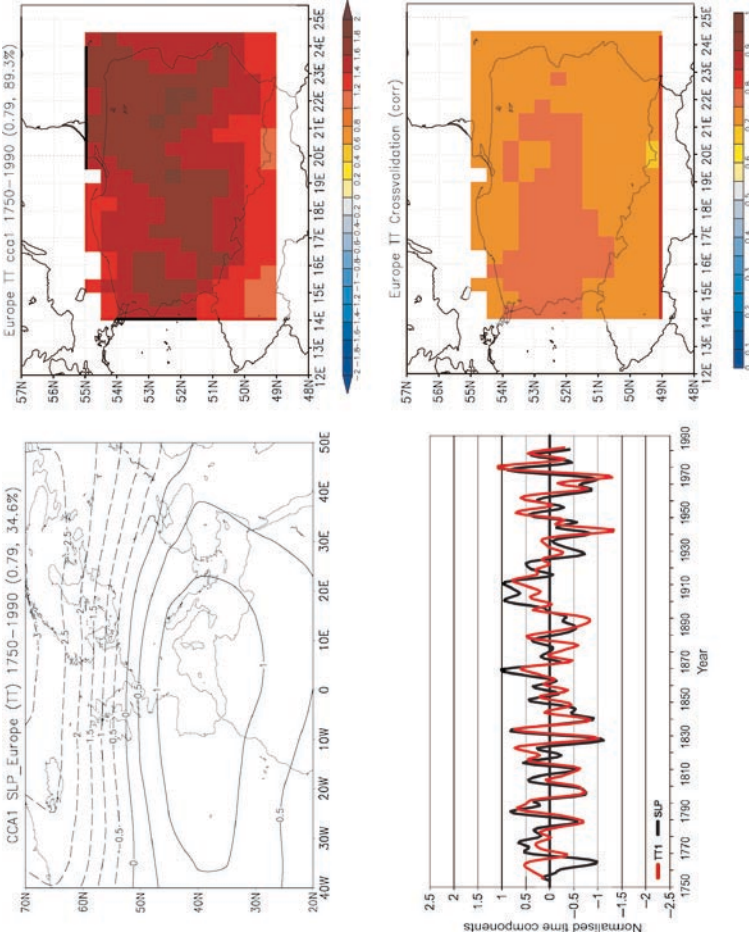


**Fig. 1.7** Canonical spatial patterns of the first CCA between winter SLP and winter gridded temperature over Poland 1750–1990 (*top right*). The canonical correlation patterns depict typical anomalies in the variables, that is hPa for SLP and °C for temperature. They explain 35% (SLP) and 89% (Polish winter temperature) of the total variance in the CCA space; (*bottom left*): normalised time components (10 year Gaussian filtered) of the first CCA patterns of SLP anomalies (*black line*) and Polish winter temperature anomalies (*red line*). The correlation between the two unfiltered winter curves is 0.79; (*bottom right*) spatial distribution of correlation obtained from cross-validation for the model using SLP as single predictor

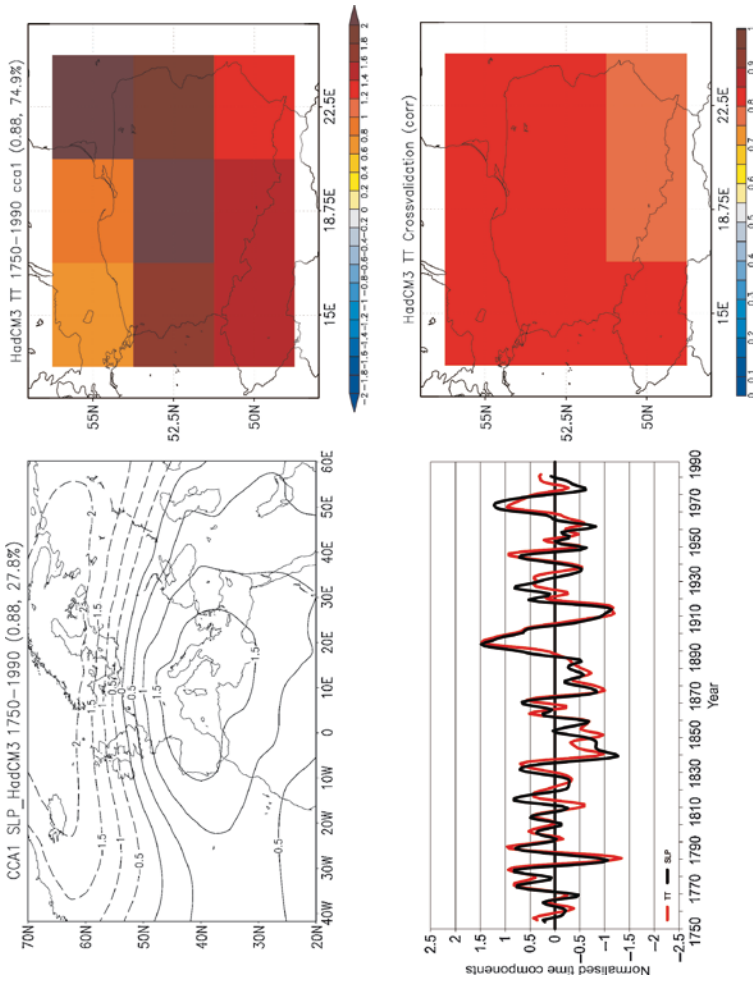


**Fig. 1.8** Same as Fig. 1.7 but for the HadCM3 model. The canonical correlation patterns account for 28% (SLP) and 75% (Polish winter temperature) of the total variance in the CCA space; (bottom left): normalised time components. The correlation between the two unfiltered winter curves is 0.88

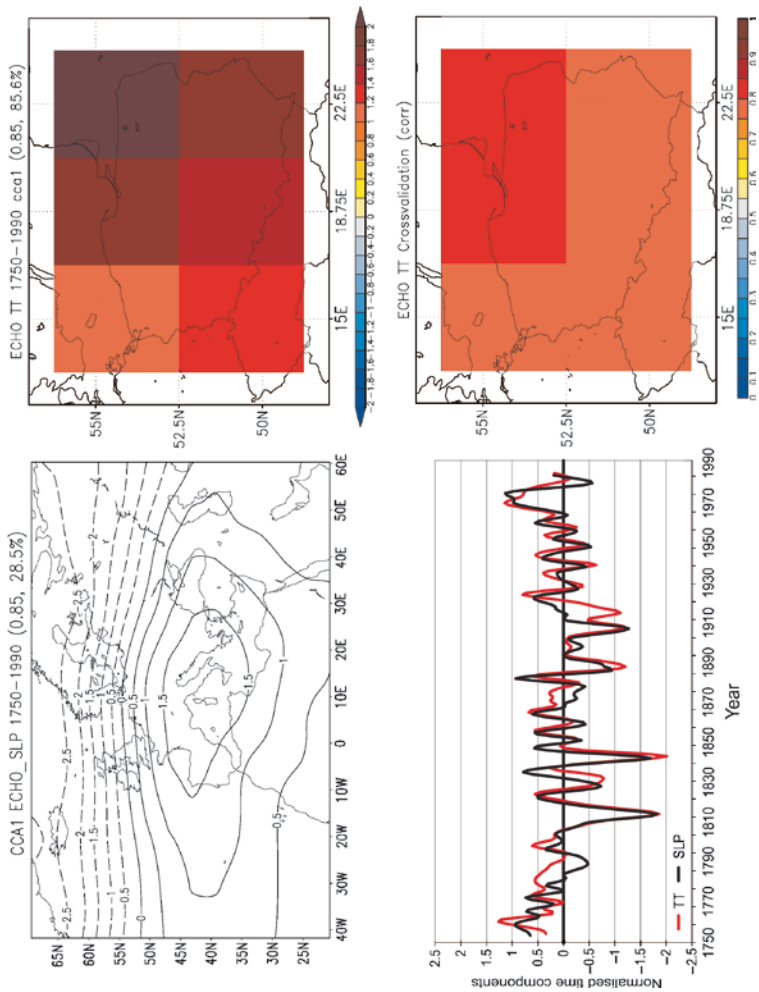


**Fig. 1.9** Same as Fig. 1.7 but for the ECHO-G model. The canonical correlation patterns account for 29% (SLP) and 86% (Polish winter temperature) of the total variance in the CCA space; (bottom left): normalised time components. The correlation between the two unfiltered winter curves is 0.85

The anomalous strong westerly flow is responsible for the positive temperature anomalies all over Poland. The normalised time components in Fig. 1.7 (bottom left) do not give any indication about long-term trends. However, distinctive decadal to interdecadal variations are visible. Figure 1.7 (bottom right) shows the spatial distribution of skill (spatial correlation) using SLP as predictor for Polish winter temperature over the last 241 years. The correlations indicate a uniform spatial structure with high values all over the country, thus the statistical downscaling model performs very well all over the grid.

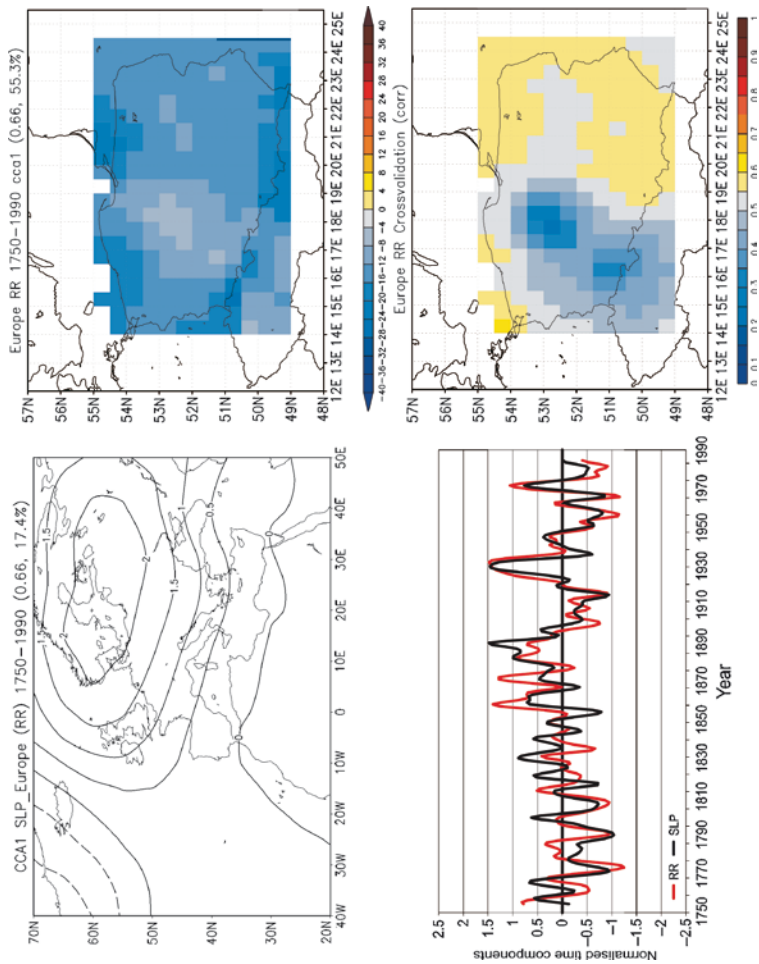
Figure 1.8 shows the first CCA pattern for the HadCM3 model. The SLP anomaly plot is very similar to the one presented in Fig. 1.7 for the reconstructions/instrumental period, both in terms of location of the anomalies as well as the pressure gradients. The corresponding anomalous temperature pattern over Poland represented by only nine grid cells support the findings from the reconstruction period with distinctly overall positive anomalies. The explained variances in the SLP and temperature fields are comparable with Fig. 1.7, though slightly lower. As for the reconstructions/instrumental CCA, there is no evidence of any trends in the normalised time components. The cross-validation results clearly indicate that the statistical downscaling model performs very well over the nine grid points.

Figure 1.9 shows the first CCA pattern for the ECHO-G model. The SLP anomaly map reveals strong resemblance to the one presented in Fig. 1.8 for the HadCM3 model and thus also for the reconstruction/instrumental period. Four out of six grid points show above normal temperature conditions. The explained variances in the SLP and temperature fields are comparable with findings from the HadCM3 and also for the reconstructions/instrumental period. As for HadCM3, there is no overall trend detectable in the normalised time components and the cross-validation results indicate very good performance over the six grid points.

Figures 1.7–1.9 reveal consistency in identifying both in the reconstructions and in the simulations the most important driving pattern of atmospheric circulation accounting for winter temperature variability over Poland. The simple mechanism behind this link highlights advection of moist mild air masses that induce higher temperatures over the study area. This atmospheric structure of low pressures over Poland also causes cloudier skies and hinders the drop of temperature that would be caused by radiative loss at night times, thus contributing to warmer winter months. The opposite can be said if the reversed sign of the pattern is considered, thus favouring continental cold air over Poland, clear skies and nocturnal radiative loss in winter.

#### 1.4.3.2 CCA SLP-Polish Winter Precipitation

The first CCA mode (Fig. 1.10, 0.66 correlation) between observed and reconstructed Polish winter precipitation and SLP (Küttel et al. 2009) during the period 1750–1990 explains around 17% of the SLP variance and more than half of the Polish winter precipitation variability. The pattern of the SLP field indicates a half-meridional positive anomaly covering large parts of the continent with the centre



**Fig. 1.10** Canonical spatial patterns of the first CCA between winter SLP (*top left*) and winter gridded precipitation over Poland 1750–1990 (*top right*). The canonical correlation patterns depict typical anomalies in the variables, that is hPa for SLP and mm for precipitation. They explain 17% (SLP) and 55% (Polish winter precipitation) of the total variance in the CCA space; (*bottom left*): normalised time components (10 year Gaussian filtered) of the first CCA patterns of SLP anomalies (*black line*) and Polish winter precipitation anomalies (*red line*). The correlation between the two unfiltered winter curves is 0.66; (*bottom right*) spatial distribution of correlation obtained from cross-validation for the model using SLP as single predictor

over southern Scandinavia. The corresponding anomalous precipitation pattern shows a monopole pattern with negative anomalies all over the country. In winters with positive normalised time components, anomalous dry air is advected from an easterly direction towards Poland. This joint pattern shows a positive trend from 1750 to the late nineteenth century (Fig. 1.10 bottom left). Within the twentieth century, the normalised time components show strong interdecadal variability with a tendency towards more anomalous low pressure conditions over northeastern Europe connected with anomalous advection of wetter conditions from the west/northwest towards Poland, in agreement with findings from Fig. 1.4. A similar analysis to that of Fig. 1.10 applied only to the 1900–1990 period leads to virtually identical results (not shown), thus suggesting that this large- to regional-scale link is stable in time.

The correlation skill score (Fig. 1.10 bottom right) generally shows higher values in the eastern part of Poland. The downscaling model performs less well in the western and southern areas.

Figure 1.11 shows the first CCA pattern between winter SLP and winter precipitation for the HadCM3 model. The SLP anomaly plot is similar to the one presented in Fig. 1.10, though with a stronger negative anomaly shifted towards the northeast. The explained variance in terms of SLP is higher than for the reconstructions/instrumental data but is smaller for the precipitation anomalies. The precipitation pattern over Poland represented by only nine grid cells connected with the dipole SLP pattern also reveals overall drier conditions (in case of positive normalised time components). No statistical long-term trend is discernible in the normalised time components, in agreement with Fig. 1.4. The cross-validation results (Fig. 1.11 bottom right) show an overall good performance of the statistical downscaling model.

Figure 1.12 presents the first CCA pattern between winter SLP and winter precipitation for the ECHO-G model. Compared to Figs. 1.10 and 1.11, the SLP anomaly pattern is more zonal with positive anomalies in the north and negative anomalies in the south (in case of positive normalised time components). The explained variances are comparable to the reconstructions/instrumental CCA (Fig. 1.10). The anomalous easterly flow connected to the positive anomaly in the north is connected with below normal precipitation over the area of Poland (Fig. 1.12 top right). There is resemblance with the overall trend of the SLP and precipitation normalised time components in Fig. 1.10, indicating an upward trend within the first 150 years approximately followed by a negative trend towards more anomalous cyclonic conditions and thus more precipitation over Poland in recent decades. The cross-validation results (Fig. 1.12 bottom right) indicate overall good performance of the statistical downscaling model.

Thus, both models show an anomalous low over the Iberian Peninsula and a relative high over Scandinavia. The impact of these simulated large-scale patterns is comparable to that found in the reconstruction where the large-scale anomaly pattern provided deficit of precipitation in the area of interest. However, the structure of the large-scale SLP pattern is somewhat different in the models and the reconstruction.

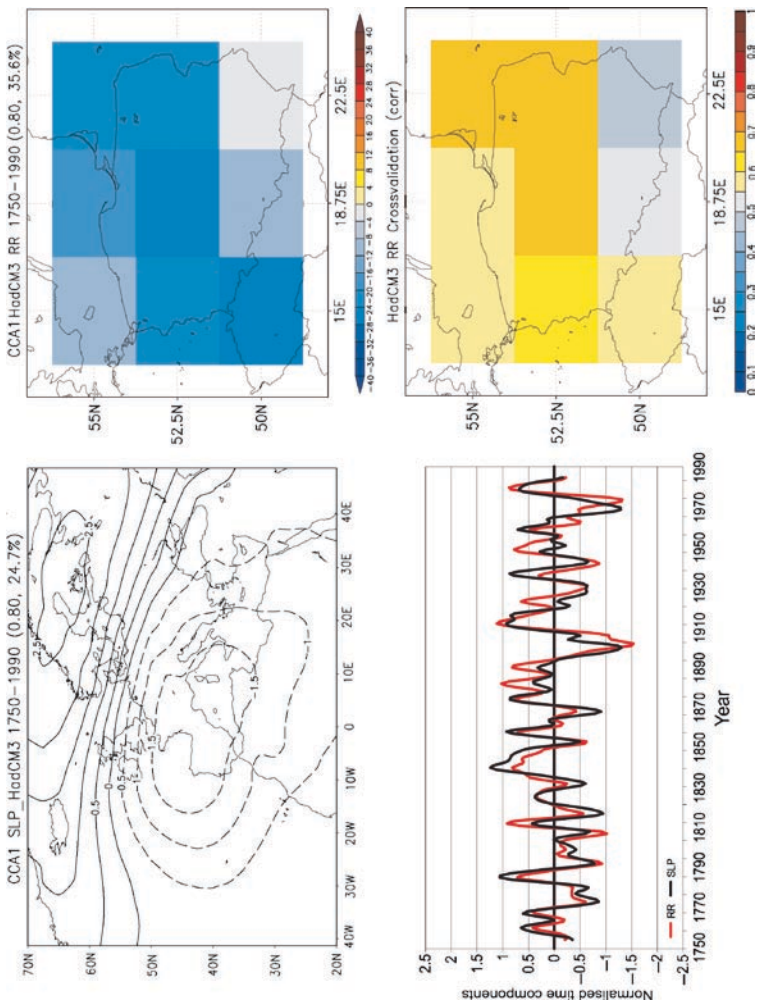


**Fig. 1.11** Same as Fig. 1.10 but for the HadCM3 model. They explain 25% (SLP) and 36% (Polish winter precipitation) of the total variance in the CCA space. The correlation between the two winter curves is 0.80



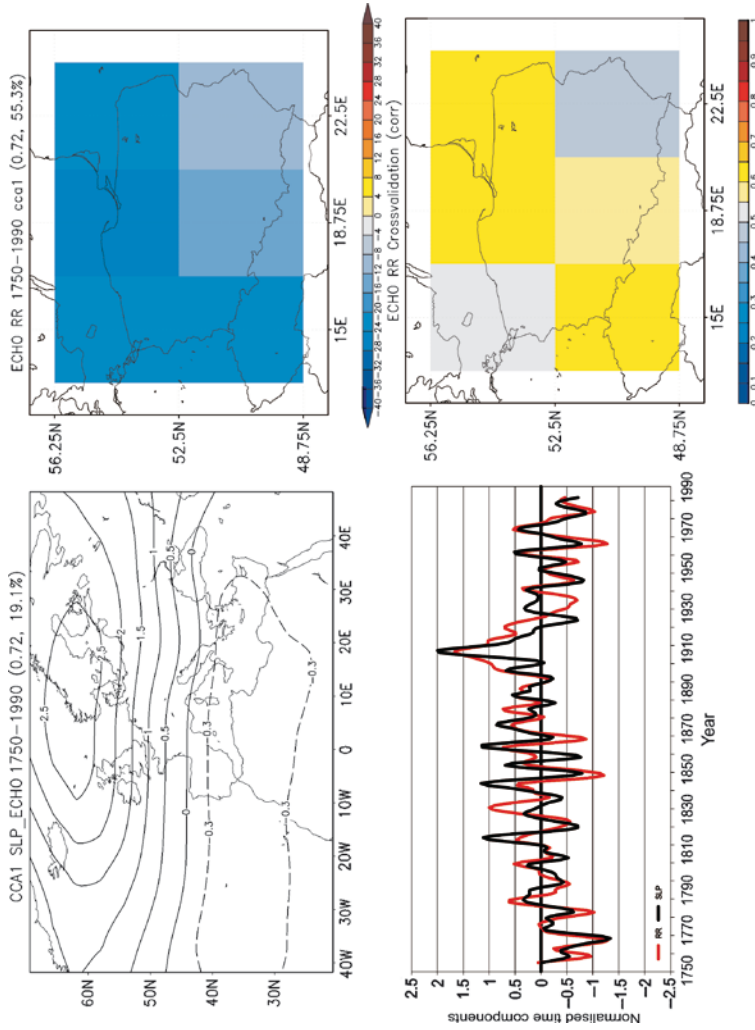


**Fig. 1.12** Same as Fig. 1.10 but for the ECHO-G model. They explain 19% (SLP) and 55% (Polish winter precipitation) of the total variance in the CCA space. The correlation between the two winter curves is 0.72

## 1.5 Discussions and Conclusions

We investigated the winter temperature and precipitation evolution over Poland over the last 500 years in comparison with the European average (excluding Poland) both in reconstructions/instrumental data and in the ECHO-G and HadCM3 models. Results indicate very good agreement between European land and Polish winter temperatures (at interannual and interdecadal time scales) both in reconstructions and in the models. In Poland, generally colder winter conditions were found within the ‘Little Ice Age’ and temperature values at the turn of the twenty first century are very likely the warmest in the context of the past half millennium. The strong agreement between Polish winter temperature and European average conditions is of major interest since some of the longest temperature proxy information stems from Poland and therefore can improve European temperature reconstructions significantly.

Precipitation is spatially and temporally more variable than temperature. However, results indicate that reconstructed winter precipitation over Poland agrees well with those of the rest of Europe. The agreement is smaller between the reconstruction and the two models. Neither the reconstructions nor the models point to significant long-term trends within the last half millennium. The low-frequency variability in the model simulations is comparable to the reconstructions, though the interannual variability is larger in both models.

The most important atmospheric circulation pattern for Polish winter temperature variability is the NAO. SCAND and to a lesser degree also the NAO and EA/WRUS are of relevance accounting for a significant amount of winter precipitation variations in Poland.

Finally, the role of the large-scale atmospheric circulation dynamics/forcing back to 1750 in explaining Polish winter temperature and precipitation variations was investigated both in the reconstructions and in the model world. CCA results show that the leading SLP modes responsible for dry/wet Polish winter conditions are in good agreement in the reconstructions and model world.

One aspect of the climate model simulations that has not received much attention so far is the amplitude of regional variations and its connections with the large-scale climate. The future global warming trend will be superimposed on multidecadal regional variability, which may be itself caused by a response to the external forcing or by the internal dynamics. An example of the first case can be illustrated by certain atmospheric circulation patterns that change with increasing concentrations of atmospheric greenhouse gases. The analyses of the model simulations indicate that the models are able to produce a quite realistic picture of the regional variability of temperature and precipitation and its connection to the continental-scale variability in this region of the midlatitudes, despite their relatively coarse resolution. The modes of atmospheric circulation relevant for regional temperature and precipitation variability are to some extent well represented in the model simulations. A stricter test on regions with more complex topography would probably be more demanding for the models, but future, higher resolutions models should be increasingly capable of producing realistic simulations of regional climate variability.

Another issue that is worth highlighting is the agreement among the CCA results between the SLP field and Polish temperature in the model simulations and in the reconstruction with those of the instrumental dataset in the twentieth century (not shown). These results suggest both that the model is able to reproduce the links observed in instrumental and proxy data and also that the large- to regional-scale relationships found in the instrumental data are robust during the last centuries of both reconstructed and simulated climate. The stability of the large- to regional-scale links is relevant not only in the context of downscaling approaches but also regarding the large-scale palaeoclimate reconstruction exercises, where the robustness of the link between a local proxy and large-scale climate is a conditional hypothesis for the reconstruction. It could be argued that since the reconstruction used herein includes the information of several modes of variability that are found in the instrumental period and used in the application of the principal component regression approach to reconstruct European past climate (e.g. Luterbacher et al. 2004; Xoplaki et al. 2005; Pauling et al. 2006), it is not surprising that the CCA analysis delivers this stable behaviour along the period of study. However, the good match with the model simulations within the multicentennial period studied suggests that the dominant mode found in the twentieth century data and in the reconstruction is also stable in the model world over the simulated period and produces similar impacts in Polish temperature.

In the case of precipitation this agreement also holds in the analysis performed on the reconstruction and on the instrumental data. As for the model, the large-scale structure found to be relevant for Polish precipitation exhibits positive pressure anomalies over Poland associated to a deficit of precipitation, as in the case of reconstruction; over southern Europe however the model suggests negative SLP anomalies, the reasons for this different behaviour remaining so far unknown.

**Acknowledgments** The contribution of Eduardo Zorita is supported by the European project Millennium (Contract no: 017008 (GOCE)). Marcel Küttel is supported by the Swiss National Science Foundation (SNSF) through its National Center of Competence in Research on Climate (NCCR Climate) project PALVAREX2 and by the European Science Foundation (ESF) activity entitled Mediterranean Climate Variability and Predictability (MedCLIVAR). This Rutishauser is supported by the Swiss National Science Foundation (SNSF). Elena Xoplaki acknowledges support by the 6th EU Framework program CIRCE (#36961). Rajmund Przybylak contribution is funded by a grant obtained from the State Committee for Scientific Research (grant no. N 306 018 32/1027), Joanna Wibigs contribution is supported by the 6th EU Framework program STATME. We thank Danuta Limanówka for important references related to earlier work on Polish weather and climate papers. We thank the Hadley Centre for the use of HadCM3 model data. We are grateful for the comments of the two anonymous reviewers.

## References

- Aasa A, Jaagus J, Ahas R, Sepp M (2004) The influence of atmospheric circulation on plant phenological phases in central and eastern Europe. *Int J Climatol* 24:1551–1564
- Ahas R, Aasa A, Menzel A, Fedotova V, Scheffinger H (2002) Changes in European spring phenology. *Int J Climatol* 22:1727–1738

- Baldini LM, McDermott F, Foley AM, Baldini JUL (2008) Spatial variability in the European winter precipitation d18O-NAO relationship: implications for reconstructing NAO-mode climate variability in the Holocene. *Geophys Res Lett* 35:L04709
- Barnett TP, Preisendorfer RW (1987) Origins and levels of monthly and seasonal forecast skill for United States air temperature determined by canonical correlation analysis. *Mon Weather Rev* 115:1825–1850
- Barnett T, Zwiers F, Hegerl G, Allen M, Crowley T, Gillett N, Hasselmann K, Jones PD, Santer B, Schnur R, Stott P, Taylor K, Tett S (2004) Detecting and attributing external influences on the climate system: a review of recent advances. *J Clim* 18:1291–1314
- Barnston AG, Livezey RE (1987) Classification, seasonality and persistence of low frequency atmospheric circulation patterns. *Mon Weather Rev* 115:1083–1126
- Bednorz E (2004) Snow cover in eastern Europe in relation to temperature, precipitation and circulation. *Int J Climatol* 24:591–601
- Bokwa A, Limanówka D, Wibig J (2001) Preinstrumental weather observations in Poland in the 16th and 17th centuries. In: Jones PD, Ogilvie AEJ, Davies TD, Briffa KR (eds) *History and climate, memories of the future*. Kluwer, New York
- Brázdil R (1996) Reconstructions of past climate from historical sources in the Czech lands. In: Jones PD, Bradley RS, Jouzel J (eds) *Climatic variations and forcing mechanisms of the last 2000 years*. Springer, Berlin/Heidelberg/New York
- Brázdil R, Dobrovolný P (2009) Historical climate in Central Europe during the last 500 years. In: Przybylak R, Majorowicz J, Brázdil R, Kejna M (eds) *The Polish climate in the European context: an historical overview*. Springer, Berlin/Heidelberg/New York
- Brázdil R, Pfister C, Wanner H, von Storch H, Luterbacher J (2005) Historical climatology in Europe – the state of the art. *Clim Change* 70:363–430
- Bujak F, (1932) *Kronika klęsk elementarnych w Polsce i Krajach sąsiednich w latach 1450–1586*. Instytut Wspierania Polskiej Twórczości Naukowej, Lwów
- Büntgen U, Frank DC, Kaczka RJ, Verstege A, Zwijacz-Kozica T, Esper J (2007) Growth responses to climate in a multi-species tree-ring network in the Western Carpathian Tatra mountains, Poland and Slovakia. *Tree Physiol* 27:689–702
- Busuioc A, von Storch H (1996) Changes in the winter precipitation in Romania and its relation to the large scale circulation. *Tellus* 48A:538–552
- Degirmendžić J, Kożuchowski K, Żmudzka E (2004) Changes of air temperature and precipitation in Poland in the period 1951–2000 and their relationship to atmospheric circulation. *Int J Climatol* 24:291–310
- Dobrovolný P, Moberg A, Brázdil R, Pfister C, Glaser R, Wilson R, van Engelen A, Limanówka D, Kiss A, Halíčková M, Macková J, Riemann D, Luterbacher J, Böhm R (2009) Monthly and seasonal temperature reconstructions for Central Europe derived from documentary evidence and instrumental records since AD 1500. *Clim Change* doi:10.1007/s10584-009-9724-x, published online 30 September 2009
- Edwards AL (1984) *An introduction to linear regression and correlation*, 2nd edn. Freeman WH, New York, pp 81–83
- Folland CK, et al. (2001) Observed climate variability and change. In: Houghton JT, et al. (eds) *Climate change 2001: the scientific basis*. Cambridge University Press, Cambridge, UK, pp 99–181
- González-Rouco JF, Beltrami H, Zorita E, von Storch H (2006) Simulation and inversion of borehole temperature profiles in surrogate climates: spatial distribution and surface coupling. *Geophys Res Lett* 33:L01703
- Guiot J, Nicault A, Rathgeber C, Edouard J, Guibal F, Pichard G, Till C (2005) Last-millennium summer-temperature variations in western Europe based on proxy data. *Holocene* 15:489–500
- Hanik J (1972) *Dzieje meteorologii i obserwacji meteorologicznych w Galicji od XVIII do XX wieku*. Zakład Narodowy im. Ossolińskich PAN, Wrocław
- Hegerl G, Zwiers FW, Braconnot P, Gillett NP, Luo Y, Marengo Orsini JA, Nicholls N, Penner JE, Stott PA (2007) Understanding and attributing climate change. In: Solomon S, et al. (eds) *Climate change 2007: the physical science basis*. Contribution of Working Group I to the Fourth

- Assessment Report of the Intergovernmental Panel on Climate Change. Cambridge University Press, Cambridge, NY, pp 663–746
- Hurrell JW (1995) Decadal trends in the North Atlantic oscillation: regional temperatures and precipitation. *Science* 269:676–679
- Jansen E, Overpeck J, Briffa KR, Duplessy JC, Joos F, Masson-Delmotte V, Olago D, Otto-Bliessner B, Peltier WR, Ramesh R, Raynaud D, Rind D, Solomina O, Villalba R, Zhang D (2007) Palaeoclimate. In: Solomon S, et al. (eds) *Climate change 2007: the physical science basis. Contribution of Working Group I to the Fourth Assessment Report of the Intergovernmental Panel on Climate Change*. Cambridge University Press, Cambridge, NY, pp 433–498
- Jones PD, Briffa KR (2006) Unusual climate in northwest Europe during the period 1730 to 1745 based on instrumental and documentary data. *Clim Change* 79:361–379
- Jones PD, Mann ME (2004) Climate over past millennia. *Rev Geophys* 42:RG2002
- Jones PD, Osborn TJ, Briffa KR (2003) Pressure-based measurements of the North Atlantic Oscillation (NAO): a comparison and an assessment of changes in the strength of the NAO and in its influence on surface climate parameters. In: Hurrell JW, Kushnir Y, Ottersen G, Visbeck M (eds) *North Atlantic oscillation: climatic significance and environmental impact*. Geophysical Monograph 134. American Geophysical Union, Washington, DC, pp 51–62
- Jones PD, Briffa KR, Osborn TJ, Lough JM, van Ommen TD, Vinther BM, Luterbacher J, Wahl E, Zwiers FW, Schmidt GA, Ammann C, Mann ME, Buckley BM, Cobb K, Esper J, Goosse H, Graham N, Jansen E, Kiefer T, Kull C, Küttel M, Mosley-Thompson E, Overpeck JT, Riedwyl N, Schulz M, Tudhope S, Villalba R, Wanner H, Wolff E, Xoplaki E (2009) High-resolution paleoclimatology of the last millennium: a review of current status and future prospects. *Holocene* 19:3–49
- Juhniewicz F, (1937) Zjawiska meteorologiczne i stan urodzajów i posuchy w Polsce w latach 1967–1750. *Sprawozdanie Towarzystwa Naukowego*, 17:63–70
- Klimenko V., and O. Solomina 2009: Climatic Variations in the East European Plain During the Last Millennium: State of the Art. In: Przybylak R, Majorowicz J, Brázdil R, Kejna M (eds) *The Polish climate in the European context: an historical overview*. Springer, Berlin/Heidelberg/New York, Doi 10.1007/978-90-481-3167-9\_3
- Küttel M, Luterbacher J, Zorita E, Xoplaki E, Riedwyl N, Wanner H (2007) Testing a European winter surface temperature reconstruction in a surrogate climate. *Geophys Res Lett* 34:L07710 doi:10.1029/2006GL027907
- Küttel M, Xoplaki E, Gallego D, Luterbacher J, Garcia-Herrera R, Allan R, Barriendos M, Jones PD, Wheeler D, Wanner H (2009) The importance of ship log data: reconstructing North Atlantic, European and Mediterranean sea level pressure fields back to 1750. *Clim Dynam* doi:10.1007/s00382-009-0577-9
- Limanówka D (1996) Daily weather observations in Cracow in the 16th century. *Zeszyty Nauk UJ, Prace Geogr* 102:503–508
- Limanówka D (2000) The transformation of thermal descriptive characteristic in Cracow from 16th century into the quantitative evaluation. *Zesz Nauk UJ, Prace Geogr* 107:113–117
- Limanówka D (2001) Rekonstrukcja warunków klimatycznych Krakowa w pierwszej połowie XVI wieku. *Mat Badaw IMGW, Seria Meteorologia* 33:3–176
- Livezey RE, Smith TM (1999) Considerations for use of the Barnett and Preisendorfer (1987) algorithm for canonical correlation analysis of climate variations. *J Clim* 12:303–305
- Lorenc H (2000) Studia nad 220-letnią (1779–1998) serią temperatury powietrza w Warszawie oraz ocena jej wiekowych tendencji. *Mat Badaw IMGW, Seria Meteorologia* 31:3–104
- Luterbacher J, Xoplaki E, Dietrich D, Rickli R, Jacobeit J, Beck C, Gyalistras D, Schmutz C, Wanner H (2002) Reconstruction of sea-level pressure fields over the Eastern North Atlantic and Europe back to 1500. *Clim Dynam* 18:545–561
- Luterbacher J, Dietrich D, Xoplaki E, Grosjean M, Wanner H (2004) European seasonal and annual temperature variability, trends, and extremes since 1500. *Science* 303:1499–1503
- Luterbacher J, Liniger MA, Menzel A, Estrella N, Della-Marta PM, Pfister C, Rutishauser T, Xoplaki E (2007) The exceptional European warmth of Autumn 2006 and Winter 2007: historical context, the underlying dynamics and its phenological impacts. *Geophys Res Lett* 34:L12704

- Luterbacher J and coauthors (2009) Circulation dynamics and influence on European and Mediterranean winter climate over the past half millennium: results and insights from instrumental data, documentary proxy evidence and coupled climate models. *Clim Change* (in press)
- Majorowicz JA (2009) The Climate of Europe in Recent Centuries in the Context of the Climate of Mid to High Latitude Northern Hemisphere from Borehole Temperature Logs. In: Przybylak R, Majorowicz J, Brázdil R, Kejna M (eds) *The Polish climate in the European context: an historical overview*. Springer, Berlin/Heidelberg/New York
- Majorowicz J, Šafanda J, Przybylak R, Wójcik G (2001) Rekonstrukcja zmian temperatury powierzchni gruntu w Polsce w ostatnim 500-leciu na podstawie profili geotermicznych. *Przeegl Geofiz* 4:305–321
- Majorowicz JA, Šafanda J, Przybylak R, Wójcik G (2004) Ground surface temperature history in Poland in the 16th–20th century derived from the inversion of geothermal profiles. *Pure Appl Geophys* 161:351–363
- Mann ME, Gille E, Bradley RS, Hughes MK, Overpeck JT, Keimig FT, Gross W (2000) Global temperature patterns in past centuries: an interactive presentation. *Earth Interact* 4:1–29
- Mann ME, Zhang Z, Hughes MK, Bradley RS, Miller SK, Rutherford S (2008) Proxy-based reconstructions of hemispheric and global surface temperature variations over the past two millennia. *Proc Natl Acad Sci USA* 105:13252–13257
- Menzel A, Sparks TH, Estrella N, Eckhardt S (2005) ‘SSW to NNE’ – North Atlantic oscillation affects the progress of seasons across Europe. *Global Change Biol* 11:909–918
- Menzel A, Sparks TH, Estrella N, Koch E, Aasa A, Ahas R, Alm-Kübler K, Bissolli P, Braslavská O, Briede A, Chmielewski FM, Crepinsek Z, Curnel Y, Dahl A, Defila C, Donnelly A, Filella I, Jatczak K, Måge F, Mestre A, Nordli Ø, Peñuelas J, Pirinen P, Remišová V, Scheffinger H, Striz M, Susnik S, Van Vliet AJH, Wielgolaski F-E, Zach S, Zust A (2006) European phenological response to climate change matches the warming pattern. *Global Change Biol* 12:1969–1976
- Michaelsen J (1987) Cross-Validation in statistical climate forecast models. *J Clim Appl Meteor* 26:1589–1600
- Mitchell T, Jones P (2005) An improved method of constructing a database of monthly climate observations and associated high-resolution grids. *Int J Climatol* 25:693–712
- Namaczyńska S (1937) Kronika klęsk elementarnych w Polsce i w krajach sąsiednich w latach 1648–1696. 1 Zjawiska meteorologiczne i pomory. *Badania z Dziejów Społecznych i Gospodarczych*, 23, Lwów
- Niedźwiedz T (1992) Kalendarz sytuacji synoptycznych dla dorzecza górnej Wisły (1986–1990). *Prace Geogr UJ* 90:71–78
- Niedźwiedz T (2004) Rekonstrukcja warunków termicznych lata w Tatrach od 1550 roku. In: Kotarba A (ed) *Rola Małej Epoki Lodowej w przekształcaniu środowiska przyrodniczego Tatr*. *Prace Geogr IGiPZ PAN* 197:57–88
- North GR, Moeng FJ, Bell TL, Cahalan RF (1982) The latitude dependence of the variance of zonally averaged quantities. *Mon Weather Rev* 110:319–326
- Osborn TJ (2004) Simulating the winter North Atlantic oscillation: the roles of internal variability and greenhouse gas forcing. *Clim Dynam* 22:605–623
- Pauling A, Luterbacher J, Casty C, Wanner H (2006) 500 years of gridded high-resolution precipitation reconstructions over Europe and the connection to large-scale circulation. *Clim Dynam* 26:387–405
- Przybylak R (2007) The change in the Polish climate in recent centuries. *Papers on Global Change IGBP* 14:7–23
- Przybylak R (2009) The climate of Poland in recent centuries: a synthesis of current knowledge: instrumental observations. In: Przybylak R, Majorowicz J, Brázdil R, Kejna M (eds) *The Polish climate in the European context: an historical overview*. Springer, Berlin/Heidelberg/New York
- Przybylak R, Wójcik G, Marciniak K (2003) Wpływ Oscylacji Północnoatlantyckiej oraz Arktycznej na warunki termiczne chłodnej pory roku w Polsce w XVI–XX wiekach. *Przeegl Geofiz* 1–2:59–72



- Przybylak R, Wójcik G, Marciniak K, Chorążyczewski W, Nowosad W, Oliński P, Syta K (2004) Zmienność warunków termiczno-opadowych w Polsce w okresie 1501–1840 w świetle danych historycznych. *Przełł Geogr* 76:5–31
- Przybylak R, Majorowicz J, Wójcik G, Zielski A, Chorążyczewski W, Marciniak K, Nowosad W, Oliński P, Syta K (2005) Temperature changes in Poland from the 16th to the 20th centuries. *Int J Climatol* 25:773–791
- Riedwyl N, Luterbacher J, Wanner H (2008) An ensemble of European summer and winter temperature reconstructions back to 1500. *Geophys Res Lett* 35:L20707
- Rojecki A (ed) (1965) Wyjątki ze źródeł historycznych o nadzwyczajnych zjawiskach hydrologiczno-meteorologicznych na ziemiach polskich w wiekach od X do XVI, Wybór i przekład na język polski: R. Girguś i W. Strupczewski. Wydawnictwa Komunikacji i Łączności, Warszawa
- Rosenzweig C, Karoly D, Vicarelli M, Neofotis P, Wu Q, Casassa G, Menzel A, Root TL, Estrella N, Séguin B, Tryjanowski P, Liu C, Rawlins S, Imeson A (2008) Attributing physical and biological impacts to anthropogenic climate change. *Nature* 453:353–357
- Rutishauser T, Luterbacher J, Defila C, Frank D, Wanner H (2008) Swiss Spring Plant Phenology 2007: extremes, a multi-century perspective and changes in temperature sensitivity. *Geophys Res Lett* 35:L05703
- Sadowski M (1991) Variability of extreme climatic events in Central Europe since the 13th century. *Zeit Meteorol* 41:350–356
- Šafanda J, Majorowicz J (2009) The climate of Poland in recent centuries – a synthesis of current knowledge: geophysical data. In: Przybylak R, Majorowicz J, Brázdil R, Keřna M (eds) *The Polish climate in the European context: an historical overview*. Springer, Berlin/Heidelberg/New York
- Scheifinger H, Menzel A, Koch E, Peter C, Ahas R (2002) Atmospheric mechanisms governing the spatial and temporal variability of phenological phases in Central Europe. *Int J Climatol* 22:1739–1755
- Sinelschikova A, Kosarev V, Panov I, Baushev AN (2007) The influence of wind conditions in Europe on the advance in timing of the spring migration of the song thrush (*Turdus philomelos*) in the south-east Baltic region. *Int J Biometeorol* 51:431–440
- Stach A, Emberlin J, Smith M, Adams-Groom B, Myszkowska D (2008) Factors that determine the severity of *Betula* spp. pollen seasons in Poland (Poznań and Cracow) and the United Kingdom (Worcester and London). *Int J Biometeorol* 52:311–321
- Stenchikov S, Hamilton K, Stouffer RJ, Robock A, Ramaswamy V, Santer B, Graf HF (2006) Arctic oscillation response to volcanic eruptions in the IPCC AR4 climate models. *J Geophys Res* 111:D07107
- Stössel M (2008) Reconstruction of precipitation in Europe: the challenge of an optimised proxy 4th November 2009 network. Diploma thesis, Institute of Geography, University of Bern, Switzerland. [http://www.giub.unibe.ch/klimet/docs/diplom\\_mstoessel.pdf](http://www.giub.unibe.ch/klimet/docs/diplom_mstoessel.pdf). Accessed on 4<sup>th</sup> November 2009
- Szewczuk J (1939) Kronika kłesk elementarnych w Galicji w latach 1772–1848. *Badania z Dziejów Społecznych i Gospodarczych* 35, Lwów
- Tett SFB, Betts R, Crowley TJ, Gregory J, Johns TC, Jones A, Osborn TJ, Öström E, Roberts DL, Woodage MJ (2007) The impact of natural and anthropogenic forcings on climate and hydrology since 1550. *Clim Dynam* 28:3–34
- Trenberth KE (1990) Recent observed interdecadal climate changes in the northern hemisphere. *Bull Am Meteorol Soc* 71:989–993
- Trenberth KE (1995) Atmospheric circulation climate changes. *Clim Change* 31:427–453
- Trepińska J (ed) (1997) *Wahania klimatu w Krakowie (1792–1995)*. Instytut Geografii UJ, Kraków
- Tryjanowski P, Kuniak S, Sparks TH (2002) Earlier arrival of some farmland migrants in western Poland. *Ibis* 144:62–68
- Tryjanowski P, Sparks TH (2008) The relationship between phenological traits and brood size of the white stork *Ciconia ciconia* in western Poland. *Acta Oecol* 33:203–206



- Twardosz R, Niedźwiedz T (2001) Influence of synoptic situations on the precipitation in Cracow (Poland). *Int J Climatol* 21:467–481
- von Storch H, Zorita E, Jones JM, Dimitriev Y, González-Rouco FJ, Tett SFB (2004) Reconstructing past climate from noisy data. *Science* 306:679–682
- von Storch H, Zwiers FW (1999) *Statistical analysis in climate research*. Cambridge University Press, Cambridge, UK
- Walawender A (1932, 1935) Kronika klęsk elementarnych w Polsce i w krajach sąsiednich w l. 1450–1586. I. Zjawiska meteorologiczne i pomory. II. Zniszczenie wojenne i pomory. *Badania z Dziejów Społecznych i Gospodarczych* 10:33–48
- Wanner H, Brönnimann S, Casty C, Gyllstras D, Luterbacher J, Schmutz C, Stephenson D, Xoplaki E (2001) North Atlantic oscillation – concept and studies. *Surv Geophys* 22:321–381
- Werchracki R (1938) Klęski elementarne w Polsce w latach 1587–1647. Cz. I. Zjawiska meteorologiczne, stan urodzajów i pomory. *Spraw Tow Nauk we Lwowie* 18(3):321–326
- Wibig J (1999) Precipitation in Europe in relation to circulation patterns at the 500 hPa level. *Int J Climatol* 19:253–269
- Wibig J (2004) Pole ciśnienia nad Europą i północnym Atlantykiem a warunki termiczne i opadowe w Polsce. In: Kożuchowski K (ed) *Skala, uwarunkowania i perspektywy współczesnych zmian klimatycznych w Polsce*. Wyd. Biblioteka, Łódź
- Wibig J (2009) The influence of atmospheric circulation on extreme weather events in Poland. Wyd. UŁ (in press)
- Wilks D (1995) *Statistical methods in the atmospheric sciences*. Academic, San Diego
- Woś A (1999) *Klimat Polski*. PWN, Warszawa
- Xoplaki E, Luterbacher J, Paeth H, Dietrich D, Steiner N, Grosjean M, Wanner H (2005) European spring and autumn temperature variability and change of extremes over the last half millennium. *Geophys Res Lett* 32:L15713